

# 1 Oscillatory and aperiodic neural activity jointly 2 predict language learning

## 3

## 4 Abbreviated Title: Neural correlates of language learning

7 Zachariah R. Cross<sup>1,\*</sup>, Andrew W. Corcoran<sup>1,2,3</sup>, Matthias Schlesewsky<sup>1</sup>, Mark. J. Kohler<sup>1,4</sup>, Ina  
8 Bornkessel-Schlesewsky<sup>1</sup>

<sup>10</sup>Cognitive Neuroscience Laboratory - Australian Research Centre for Interactive and Virtual  
<sup>11</sup>Environments, University of South Australia, Adelaide, Australia.

<sup>12</sup>Cognition and Philosophy Laboratory, Monash University, Melbourne, Australia.

<sup>3</sup>Monash Centre for Consciousness & Contemplative Studies, Monash University, Melbourne, Australia.

14 <sup>4</sup>Faculty of Health and Medical Sciences, Adelaide University, Adelaide, Australia.

**Corresponding author:** Zachariah R. Cross, Room H1-06C, University of South Australia Magill Campus, St Bernards Road, Magill, SA 5072, Australia. E-mail: Zachariah.Cross@unisa.edu.au

## 22 Manuscript details

22 Manuscript details  
23 Number of pages: 41

24 Number of figures: 8

25 Abstract word count: 201

26 Introduction word count: 678

27 Discussion word count: 2,687

28 Data and code available at: <https://osf.io/7yr46/>

31 **Acknowledgements:** Preparation of this work was supported by Australian Commonwealth  
32 Government funding awarded to ZRC and AWC under the Research Training Program. IB-S is  
33 supported by an Australian Research Council Future Fellowship (FT160100437). AWC is supported  
34 by the Three Springs Foundation. We thank Isabella Sharrad, Lena Zou-Williams, Erica Wilkinson,  
35 Nicole Vass and Angela Osborn for help with data collection. Thank you also to the participants.

**Conflict of interest statement:** The authors declare no competing financial interests.

50

## Abstract

51 Memory formation involves the synchronous firing of neurons in task-relevant networks, with recent  
52 models postulating that a decrease in low frequency oscillatory activity underlies successful memory  
53 encoding and retrieval. However, to date, this relationship has been investigated primarily with face  
54 and image stimuli; considerably less is known about the oscillatory correlates of complex rule learning,  
55 as in language. Further, recent work has shown that non-oscillatory (1/f) activity is functionally relevant  
56 to cognition, yet its interaction with oscillatory activity during complex rule learning remains unknown.  
57 Using spectral decomposition and power-law exponent estimation of human EEG data (17 females, 18  
58 males), we show for the first time that 1/f and oscillatory activity jointly influence the learning of word  
59 order rules of a miniature artificial language system. Flexible word order rules were associated with a  
60 steeper 1/f slope, while fixed word order rules were associated with a shallower slope. We also show  
61 that increased theta and alpha power predicts fixed relative to flexible word order rule learning and  
62 behavioural performance. Together, these results suggest that 1/f activity plays an important role in  
63 higher-order cognition, including language processing, and that grammar learning is modulated by  
64 different word order permutations, which manifest in distinct oscillatory profiles.

65

66

67

68

69

70

71

72 **Keywords:** language learning • neural oscillations • aperiodic activity • sentence processing • EEG •  
73 artificial grammar

74

75

76

77

78

## Introduction

79 Memory supports many essential cognitive functions, from learning the distinction between  
80 semantic categories (e.g., animal vs. human) to complex (motor) sequences, such as learning how to  
81 drive a car or speak a new language. However, while a broad literature has related neural oscillatory  
82 dynamics (i.e., [de]synchronisation of neural populations) to the encoding and retrieval of images and  
83 words (e.g., Parish, Hanslmayr, & Bowman, 2018), considerably less is known about oscillatory activity  
84 during the encoding and retrieval of complex sequences, such as in language (cf. de Diego-Balaguer,  
85 Fuentemilla, & Rodriguez-Fornells, 2011; Kepinska, Pereda, Caspers, & Schiller, 2017). Further, the  
86 few studies examining sequence and artificial language learning report mixed findings relative to  
87 (episodic) word and image paradigms: while alpha/beta desynchronisation in the human EEG predicts  
88 encoding of words and images (e.g., Griffiths, et al., 2019), alpha/beta and theta synchronisation is  
89 associated with sequence (Crivelli-Decker et al., 2018) and language learning (e.g., Kepinska et al.,  
90 2017). This apparent inconsistency might be accounted for by stimulus heterogeneity; however, another  
91 possible source of divergence may lie in the mixture of oscillatory power with aperiodic activity  
92 (Ouyang et al., 2020; Wen & Liu, 2016), which has not been addressed in studies on the neural basis of  
93 complex rule learning to date.

94 Electrophysiological brain activity exhibits a  $1/f$ -like power distribution, which is often  
95 removed from the signal to isolate transient task-related oscillations (Donoghue et al., 2020; He, 2014;  
96 Lendner et al., 2020). However, this aperiodic component has recently been implicated in a variety of  
97 higher-order cognitive computations (Fellner et al., 2019), partially explaining individual differences  
98 in theta activity during memory encoding and recall performance (Sheehan et al., 2018), and processing  
99 speed over and above that of alpha activity (Ouyang et al., 2020). Work on prediction during language  
100 has also shown that the aperiodic slope – but not oscillatory activity – influences the N400 event-related  
101 potential and performance accuracy (Dave et al., 2018).

102 These findings suggest that aperiodic brain activity plays a critical functional role in the  
103 neurobiology of cognition (He et al., 2010); however, it is currently unknown whether oscillatory and  
104 aperiodic activity interact during memory encoding of information beyond single words and images,  
105 such as rule-based sequence learning, and whether any such interaction influences behavioural

106 outcomes. Clarifying the (separable) roles of oscillatory and aperiodic components of the EEG power  
107 spectrum may also bridge diverging results reported in studies using image and word stimuli and  
108 artificial grammar paradigms, lending support to the idea that neural oscillations differentially  
109 contribute to memory formation.

110 To better characterise the neural mechanisms underlying complex rule learning, we examined  
111 fluctuations in delta, theta, alpha and beta power during an artificial language learning task. We also  
112 modelled the interaction between oscillatory and aperiodic activity to characterise how patterns of  
113 (de)synchronisation and aperiodic fluctuation influence the generalisation of different word order rules  
114 characteristic of many natural languages. Healthy young adults learned the artificial miniature language  
115 Mini Pinyin (Cross, Zou-Williams, Wilkinson, Schlesewsky, & Bornkessel-Schlesewsky, 2020a)  
116 without explicit instruction and then completed a sentence judgement task. Critically, participants –  
117 who were native monolingual English speakers – learned fixed and flexible word order rules: fixed  
118 word order sentences contained temporal- or sequence-based rules, while flexible word order sentences  
119 involved non-adjacent dependencies, likely relying on more associative- than sequence-based memory  
120 processing mechanisms (Cross et al., 2018). From this perspective, we were able to probe different  
121 learning and memory mechanisms that are involved in sentence comprehension (Bornkessel-  
122 Schlesewsky, Schlesewsky et al., 2015). For example, native English speakers typically rely on word-  
123 order-based cues for sentence comprehension, whereas speakers of Mandarin Chinese or the Australian  
124 language Jiwarli rely more strongly on cues other than word order, such as case marking and/or  
125 semantic information, including animacy (Austin, 2001; Bates et al., 2001; Bornkessel-Schlesewsky et  
126 al., 2011).

127 We recorded EEG during the learning task, implementing generalised additive and linear  
128 mixed-effects regression analyses to model dynamic changes in oscillatory and aperiodic activity during  
129 the learning of the fixed and flexible word order rules. We also modelled learning-related oscillatory  
130 and aperiodic activity to predict subsequent behavioural performance on the sentence judgement task,  
131 quantified as the sensitivity index  $d'$ .

132

133

134

## Method

135 **Participants**

136 Data from 36 right-handed healthy, monolingual, native English-speakers were used from a  
137 study examining the effect of sleep on language learning (Cross et al., 2021). This sample size was  
138 based on previous EEG research examining the neural correlates of higher-order language learning (de  
139 Diego-Balaguer et al., 2011; Kepinska et al., 2017; Mueller et al., 2005). One participant was excluded  
140 from analysis for not having electroencephalography recorded during the sentence learning task due to  
141 experimenter error. The final sample size was 35 ( $M_{age} = 25.3$ ,  $SD = 7.13$ ; 17 female). Ethics approval  
142 was granted by the University of South Australia's Human Research Ethics committee (I.D.:  
143 0000032556).

144 **Stimuli and experimental design**

145 Stimuli were based on the modified miniature language Mini Pinyin (for a detailed description  
146 of the language, see Cross et al., 2020a; see also Cross et al., 2021), which contains grammatical rules  
147 present in a number of natural languages (see Figure 1A and 1B for example sentence constructions  
148 and vocabulary items). Briefly, each sentence in Mini Pinyin contains two noun phrases and a verb, and  
149 each noun is associated with a different classifier: human nouns are preceded by *ge*, while animals, and  
150 small and large objects are preceded by *zhi*, *xi* and *da*, respectively.

151 Mini Pinyin includes two main sentence types based on whether the sentence contains the  
152 coverbs *ba* and *bei*. Here we focus on the coverb *ba*: when *ba* is present, the sentence contains a fixed  
153 word order, in that the first noun phrase is invariably the Actor (the active, controlling participant in the  
154 action described by the sentence) and the sentence must be verb final. In this context, accurate sentence  
155 processing is dependent on the linear position of the words. When *ba* is not present, the sentence  
156 contains a flexible word order, in that the first noun phrase can either be the Actor or the Undergoer  
157 (the affected participant); however, the sentence must be verb-medial (i.e., verb must be positioned  
158 between the noun phrases). As such, accurate sentence interpretation is based more heavily on the

159 animacy status of the noun phrases rather than word order. These manipulations are illustrated below,  
160 with a flexible word order shown in 1a and 1b and fixed (i.e., with the coverb *ba*) shown in 2:

161 (1)

162 (a) ge yisheng dale da piqu.  
163 (human) doctor hit (object) ball.  
164 “the doctor hits the ball.”  
165 (b) da xianjiao chile zhi laoshu.  
166 (object) banana eat (animal) rat.  
167 “the rat eats the banana.”

168 (2)

169 ge xiaofang ba da shubao liangle.  
170 (human) firefighter ba (object) bag measure.  
171 “the firefighter measures the bag.”

172  
173 The experiment contained three phases: a vocabulary test, a learning phase, and a  
174 grammaticality judgement task. Approximately seven days before the sentence learning phase,  
175 participants received a paired picture-word vocabulary booklet containing the 25 nouns. Participants  
176 were required to learn the 25 nouns to ensure that they had a basic vocabulary. Prior to the learning and  
177 judgement tasks, participants completed the vocabulary test on a desktop computer by typing in  
178 translations of the nouns from Mini Pinyin to English. Only participants who attained a score > 90%  
179 were eligible to undertake the learning and judgement task phases of the experiment. All 35 participants  
180 achieved 90% accuracy on the vocabulary task and thus completed the main experimental session.  
181 Overall, 576 unique sentences (288 grammatical, 288 ungrammatical) were created and divided into  
182 two equivalent sets.

183 We focus here on a subset of sentence conditions to investigate the mechanisms underlying the  
184 learning of different word order permutations (for EEG analyses during the sentence judgement task,  
185 see Cross et al., 2021). While no explicit instructions were given to participants in regard to the structure  
186 of the miniature language, a picture was shown prior to each sentence illustrating an event occurring  
187 between two entities, which was then described in the subsequently presented sentence. The learning

188 task contained four blocks with 128 grammatical picture-sentence pairs overall (96 of which were  
189 included in the subset analysed here) that were presented via rapid visual serial presentation. The subset  
190 contained a further 156 novel sentences (50% grammatical, 50% ungrammatical) that were presented  
191 during the judgement task, which occurred immediately after the learning phase. The remaining  
192 sentences were considered fillers. The ungrammatical sentences induced a violation at either the  
193 position of the Actor or verb in fixed word order sentences (e.g., Actor-ba-Verb-Undergoer [AbaVU]  
194 instead of AbaUV) or the position of the verb in flexible word order sentences (e.g., AUV instead of  
195 AVU; see Figure 1A for an illustration and full list of ungrammatical constructions).

196 During the learning phase, each picture was presented for 5000ms, while each corresponding  
197 sentence was presented on a word-by-word basis, with each word presented for 700ms with an inter-  
198 stimulus interval (ISI) of 200ms. Across the four blocks, each grammatical construction was presented  
199 32 times, with stimuli pseudo-randomised such that no sentences of the same construction followed  
200 each other. During the judgement task, novel grammatical and ungrammatical sentences were presented  
201 word-by-word with a presentation time of 600ms and an ISI of 200ms. Participants responded via a  
202 button press to indicate whether the sentence conformed to the rules of Mini Pinyin. The assignment of  
203 grammatical/ungrammatical response buttons was counterbalanced across participants. Response time  
204 windows were presented for a maximum of 4000ms. Participants received feedback on whether their  
205 response was correct or incorrect (see Figure 1C and 1D for a schematic of the learning and judgement  
206 tasks, respectively). Both the learning and judgement tasks were created in OpenSesame (Mathot et al.,  
207 2012) and performed on a desktop computer.

### (A) Grammatical and Ungrammatical Sentence Constructions

#### Grammatical:

AVU: ge shuishou **zhuole** zhi maomi  
UVA: zhi maomi **zhuole** ge shuishou  
AbaUV: ge shuishou **ba** zhi maomi **zhuole**

English Translation: the sailor **captures** the cat

#### Ungrammatical:

UbaAV: zhi maomi **ba** ge shuishou **zhuole**  
AbaVU: ge shuishou **ba** **zhuole** zhi maomi  
AUV: ge shuishou zhi maomi **zhuole**  
UAV: zhi maomi ge shuishou **zhuole**

### (B) Sample of Linguistic Elements from Mini Pinyin and English Translations

#### Classifier

: ge (human), zhi (animal), da (large object), xi (small object)

#### Noun

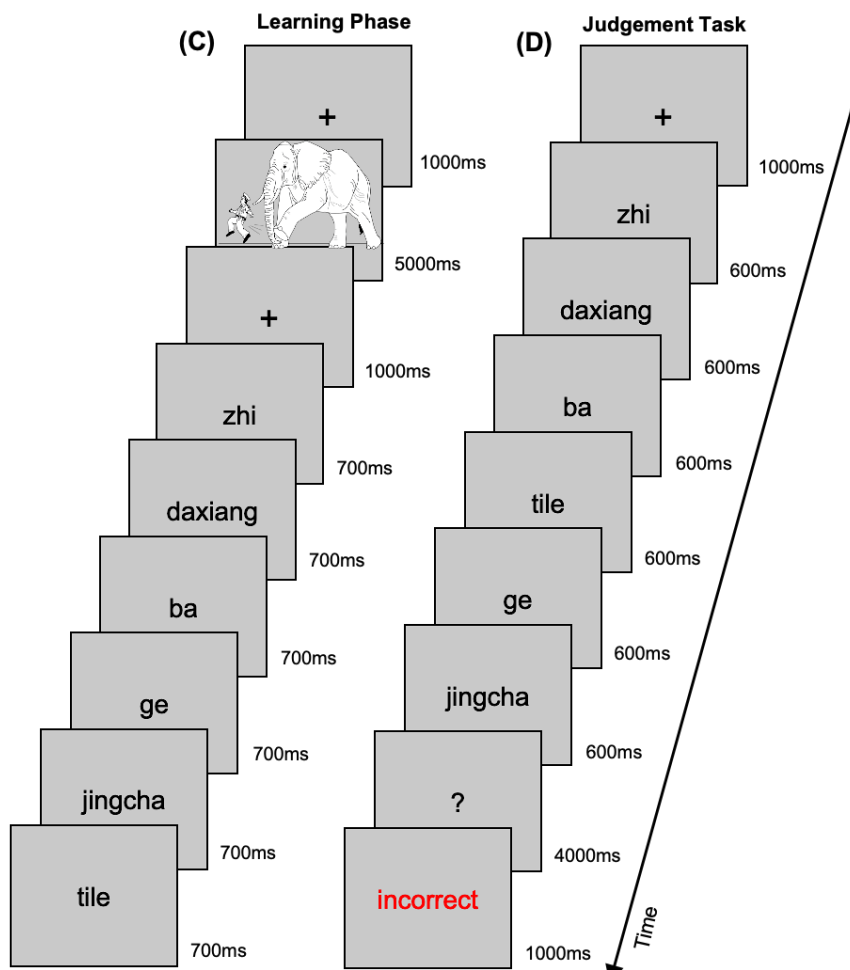
: shuishou (sailor), maomi (cat), junma (pirate), pingguo (apple)

#### Coverb

: ba (actor-undergoer-verb)

#### Verb

: zhule (capture), xile (wash), zhao (photograph), chile (eat)



208

209 **Figure 1.** (A) Summary of the grammatical (left) and ungrammatical (right) sentence constructions. (B)  
210 A portion of linguistic elements used in the sentence examples provided in (A). (C) Schematic of the  
211 sequence of events occurring in the sentence learning phase. (D) Schematic of the sequence of events  
212 occurring in the sentence judgement task.

213

214

215

216 **EEG recording and pre-processing**

217 Participants' EEG was recorded using a 32-channel BrainCap with sintered Ag/AgCl electrodes  
218 (Brain Products, GmbH, Gilching, Germany) mounted according to the extended International 10-20  
219 system. The online reference was located at FCz. The ground electrode was located at AFz. The  
220 electrooculogram (EOG) was recorded via electrodes located at the outer canthus of each eye and above  
221 and below participants' left eye. The EEG was amplified using a BrainAmp DC amplifier (Brain  
222 Products GmbH, Gilching, Germany) with an initial band-pass filter of DC – 250 Hz and a sampling  
223 rate of 1000 Hz. Electrode impedances were kept below 10kΩ. EEG was also recorded during two  
224 minutes of eyes-open and two minutes of eyes-closed resting-state periods immediately before the  
225 learning task and after the judgement task.

226 EEG analysis was performed in MATLAB 2017b (The MathWorks, Natick, USA) using  
227 custom scripts in conjunction with the Fieldtrip toolbox (Oostenveld et al., 2011). EEG data were re-  
228 referenced offline to the average of both mastoids and band-pass filtered from 1 – 40 Hz using a two-  
229 pass Butterworth IIR filter (implemented in ft\_preprocessing). Data were then epoched from -200ms to  
230 13s relative to the onset of each picture-sentence pair for both fixed and flexible sentences, and  
231 corrected for ocular artefacts using Infomax Independent Component Analysis (Bell & Sejnowski,  
232 1995; implemented in runica.m). Components demonstrating clear EOG artefacts were removed  
233 (median components rejected = 3, range = 2 – 6) and electrodes showing strong artefacts were visually  
234 inspected and subsequently interpolated with surrounding electrodes based on spherical spline  
235 interpolation (total channels interpolated  $n = 2$ ; Perrin et al., 1989).

236 **EEG data analysis**

237 The aim of the analysis was to characterise the oscillatory and aperiodic dynamics underlying  
238 the initial encoding of complex grammatical rules. To this end, we computed differences between fixed  
239 and flexible word order sentences in the following five spectral features of the EEG recorded during  
240 the learning phase: mean power density within individualised delta, theta, alpha, and beta bands, and  
241 the (inverse) slope of the  $1/f$  spectral distribution (i.e., power-law exponent). We then used these

242 metrics to investigate whether trial-level variation in oscillatory power and  $1/f$  slope during the learning  
243 task predicted behavioural performance on the judgement task. We also tested whether interactions  
244 between oscillatory and aperiodic activity afford unique information predicting behavioural  
245 performance.

246 *Spectral decomposition and power-law exponent  $\chi$  estimation*

247 The power-law scaling exponent  $\chi$ , which summarises the rate of decay of the power spectrum  
248 in double-logarithmic co-ordinates, was estimated using the Irregular-Resampling Auto-Spectral  
249 Analysis toolbox (IRASA v1.0; Wen & Liu, 2016). Briefly, this technique seeks to separate oscillatory  
250 from aperiodic (random fractal) components by iteratively resampling the power spectrum across a  
251 range of non-integer factors  $h$  and their reciprocals  $1/h$  (here,  $h = 1.1$  to  $1.95$  in steps of  $0.05$ ). This  
252 procedure shifts any narrowband components away from their original location along the frequency  
253 spectrum while leaving the distribution of the fractal component intact. The median of the resampled  
254 spectral estimates is then calculated in order to strip the spectrum of narrowband peaks. For a more  
255 detailed treatment of the IRASA method, see Wen and Liu (2016).

256 Trial data from each EEG channel were divided into two non-overlapping 4500ms segments  
257 corresponding to the picture and sentence presentation phases, respectively. Picture segments were  
258 timelocked to 500ms post-stimulus onset; sentence segments were timelocked to 100 ms prior to the  
259 first word onset. Both segments were further subdivided into seven 1800ms epochs (25% overlap) and  
260 separately passed to `amri_sig_fractal.m` for spectral parameter estimation. Once the fractal component  
261 had been recovered from each power spectrum, it was parameterised using `amri_sig_plawfit.m`. This  
262 function rescales the frequency spectrum to achieve equally-spaced intervals in log-space before fitting  
263 a linear regression to a subregion of the double-log transformed fractal spectrum (here,  $\sim 1.9 - 15.8$  Hz,  
264 corresponding to an evaluated frequency range of 1 – 35 Hz; see Gerster et al. 2022, for further details).  
265 The absolute value of the regression slope coefficient was taken as the  $\chi$  exponent.

266 To ensure the robustness of our analysis, we compared our estimates of the  $\chi$  exponent against  
267 those derived using the more recently-developed ‘FOOOF’ method (Donoghue et al., 2020). Briefly,  
268 this technique attempts to separate narrowband oscillatory peak components from broadband aperiodic

269 activity by iteratively fitting Gaussian functions to the spectrum, and deleting these components until  
270 no further deviations from background activity can be detected (given a predefined noise threshold).  
271 The  $\chi$  exponent is then estimated by fitting a regression to the residual spectrum in double-log space,  
272 similar to the IRASA procedure (see Donoghue et al., 2020, for details).

273 Since FOOOF requires PSD estimates (rather than timeseries data) as its input, power spectra  
274 were derived from each epoch using the pwelch.m implementation of Welch's (1967) modified  
275 periodogram method. Epochs were Hann-tapered and zero-padded to 2048 points to facilitate  
276 comparability with IRASA-generated spectral estimates. FOOOF was implemented via the MATLAB  
277 wrapper (v1.0.0) using the following parameter settings: peak width limits = 1 – 12 Hz, maximum  
278 number of peaks = infinite, minimum peak height = 0, peak threshold = 2 S.D., aperiodic mode = fixed,  
279 evaluated frequency range = 1 – 35 Hz.

280 *Spectral band power estimation*

281 In order to quantify narrowband changes in spectral power independent of underlying changes  
282 in aperiodic activity, mean power densities were estimated following the subtraction of the mean  
283 regression fit of the aperiodic component from the PSD (spectra averaged across epochs within each  
284 segment). This residual, ‘oscillatory’ spectrum was half-wave rectified (negative values set to zero) and  
285 divided into the four frequency bands of interest. Notably, the limits of each frequency band were  
286 adapted for each participant on the basis of their resting-state EEG. Specifically, the boundaries of each  
287 frequency band were calculated according to the harmonic frequency architecture proposed by  
288 Klimesch (2012; 2013; and which is in line with previous work, e.g., Corcoran et al., 2018, Doppelmayr  
289 et al., 1998, Sauppe et al., 2021), in which the centre frequency of each successive band constitutes a  
290 harmonic series scaled in relation to the individual alpha frequency (IAF). To avoid the potential overlap  
291 of neighbouring frequency bands, we determined lower and upper frequency bounds using the  
292 following formulae:

293 
$$f_1 = f_c - f_c/4,$$

294 
$$f_2 = f_c + f_c/2,$$

295 where  $f_c$  is the centre frequency (based on the IAF-scaled harmonic series),  $f_1$  the lower bound, and  $f_2$   
296 the higher bound of a given frequency band.

297 IAF estimates used to determine  $f_c$  were obtained from a set of parieto-occipital electrodes  
298 (P3/P4/O1/O2/P7/P8/Pz/Iz) using the *restingIAF* package (v1.0.3; Corcoran et al., 2019; see also Cross  
299 et al. 2020b). This method applies a Savitzky-Golay filter (frame width = 11 bins, polynomial order =  
300 5) to smooth and differentiate the power spectrum prior to estimating the peak frequency within a  
301 specified frequency range (here, 7—14 Hz). Peak estimates were averaged across channels, with a  
302 minimum of 3 channel estimates required to return an IAF for a given recording. Estimates derived  
303 from pre- and post-session eyes-closed resting states were then averaged for each participant using  
304 *meanIAF.m*. For further details on this algorithm, see Corcoran and colleagues (2018).

305 Having determined IAF-anchored bounds for the delta, theta, alpha, and beta bands, power  
306 within each band was quantified using the mean power density metric proposed by Westfall (1990):

$$307 P_k = \frac{1}{1 + k_{f_2} - k_{f_1}} \sum_{i=k_{f_1}}^{k_{f_2}} p(f_i),$$

308 where  $p(f_i)$  is the power estimate of the  $i^{\text{th}}$  frequency bin, and  $f_1$  and  $f_2$  index the lower and upper bounds  
309 of the individualised frequency band  $k$ , respectively. An advantage of this approach is that power  
310 estimates are scaled by spectral range, thus controlling for differing frequency bandwidths both within  
311 and between individuals.

## 312 **Statistical analysis**

313 We used *R* v.4.0.0 (R Core Team, 2020) and the packages *lme4* v.1.1.27.1 (Bates et al., 2015),  
314 *lmerTest* v.3.1.2 (Kuznetsova et al., 2017), *ggeffects* v.4.1.4 (Lüdecke, 2018), *car* v.3.0.7 (Fox et al.,  
315 2011), *tidyverse* v.1.3.0 (Wickham et al., 2019), *mgcv* v.1.8.36 (Wood, 2006), *mgcViz* v.0.1.9 (Fasiolo  
316 et al., 2019), *rgl* v.0.1.54 (Nenadic & Greenacre, 2007), *ggpubr* v.0.4.0 (Kassambara (2020), *cowplot*  
317 v.1.0.0 (Wilke, 2019), and *eegUtils* v.0.7.0 (Craddock, 2022). For linear models, contrasts for  
318 categorical variables were sum-to-zero contrast coded, with coefficients reflecting deviation from the  
319 grand mean (Schad et al., 2020).

320

321

322 *Generalised additive mixed models*

323 Generalized additive models (GAMs) are a nonparametric extension of the standard linear  
324 regression model that substitute a linear predictor variable  $x$  with a smooth function  $f(x)$  (Hastie &  
325 Tibshirani, 1987, 1990; Wood, 2017). Generalized additive mixed models (GAMMs; Lin & Zhang,  
326 1999) constitute a further extension that incorporates random effects components within the GAM  
327 framework (Pedersen et al., 2019). Together, these innovations offer an elegant solution to the problem  
328 of autocorrelation amongst residuals induced by (1) attempting to fit linear models to non-linear  
329 relationships, and (2) non-independence (or nesting) of observations (e.g., repeated measures within  
330 participants or items; Baayen et al., 2008).

331 Here, GAMMs were constructed to investigate how the exponent  $\chi$ , and the mean power density  
332  $P$  for each  $k^{\text{th}}$  frequency band (delta, theta, alpha, and beta), fluctuate during artificial grammar learning.  
333 Trial-level  $\chi$  and  $P_k$  estimates from the sentence processing phase of each trial were modelled as a  
334 function of learning time (trial number), sensor space (2D Cartesian co-ordinates), and sentence type  
335 (fixed, flexible). Estimates from the preceding image presentation phase were treated as a baseline  
336 measure of spectral activity. Random factor smooth interactions were included to account for individual  
337 differences in the functional relationship between spectral features and time-on-task (see Baayen et al.,  
338 2017, Corcoran, Macefield, & Hohwy, 2021, for similar approaches). Each GAMM took the following  
339 general form:

$$340 \quad Y_i = \beta_0 + \beta_1 type_i + \beta_2 baseline_i + f(trial_i, topo.x_i, topo.y_i, by = type_i) + \\ 341 \quad f_{subject_i}(time) + \epsilon,$$

342 where  $Y_i$  is the  $i^{\text{th}}$  observation of spectral feature  $Y$ ,  $\beta_0$  is the model intercept,  $\beta_1 type$  is a factor encoding  
343 the main effect of Sentence Type,  $\beta_2 baseline$  is a covariate encoding the corresponding observation for  
344  $Y$  during the baseline period,  $f(\cdot, by = type)$  is the tensor product interaction between the learning time  
345 ( $trial$ ) and sensor space ( $topo.x, topo.y$ ) covariates for each level of Sentence Type,  $f_{subject}$  is the by-  
346 participant factor smooth for time-on-task, and  $\epsilon$  is a  $t$  distributed error term (since response variables  
347 were heavy-tailed). Note that marginal smooths for sensor space co-ordinates were treated as isotropic  
348 (i.e., assumed to share a common scale).

349 GAMMs were estimated using the `bam()` function of the *R* package `mgcv` (Wood, 2011).  
350 Models were fit using the Fast REML method.  $P_k$  estimates for both the baseline and sentence  
351 processing period were  $\log_{10}$  transformed prior to model inclusion. Models were fit with tensor product  
352 interaction smooths in order to enable ANOVA-decomposition of main effect and interaction  
353 components (Wood, Scheipl, & Faraway, 2013). All tensor product smooths were fit using low rank  
354 thin plate regression splines as their basis function (Wood, 2003, 2017). Factor smooths were fit with a  
355 first-derivative penalty in order to shrink participant-level smooths towards the population-level. An  
356 additional shrinkage penalty was imposed on the smoothing penalty null space to enable automated  
357 model reduction (see Marra & Wood, 2011). Type was entered as an ordered factor with Fixed assigned  
358 as the reference level, hence model terms involving a Sentence Type interaction assess the difference  
359 between Fixed and Flexible condition splines (see van Rij et al., 2016).

360 *Linear mixed-effects models*

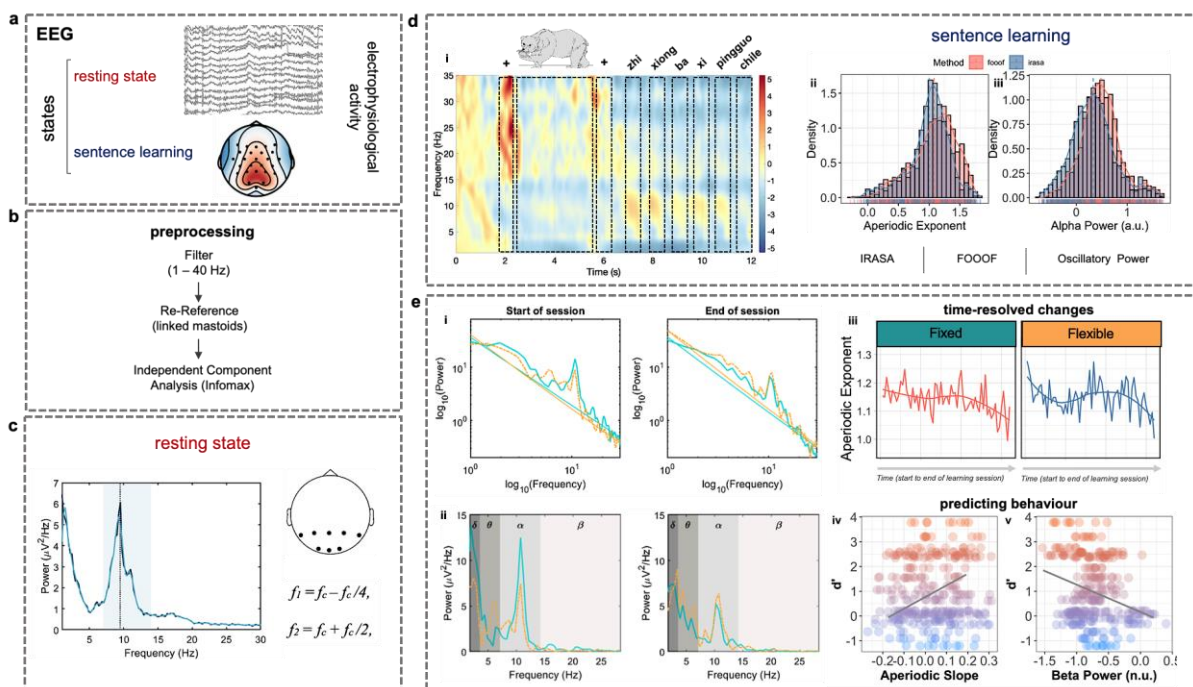
361 The relationship between aperiodic and oscillatory power during grammar learning with  
362 behavioural performance on the judgement task was assessed using linear mixed-effects models.  
363 Behavioural performance was operationalised using the discrimination index ( $d'$ ).  $d'$  is defined as the  
364 difference between the  $z$  transformed probabilities of hit rate (HR) and false alarm rate (FA; i.e.,  
365  $d' = z[HR] - z[FA]$ ). These models took the following general form:

366 
$$d'_i = \beta_0 + \beta_1 P_{k_i} * \beta_2 bexp_i * \beta_3 type_i * \beta_4 lat_i * \beta_5 sag_i + participant_{0i} + \epsilon,$$

367 where  $P_k$  is mean baseline-corrected (i.e., sentence presentation – pre-sentence interval) power density  
368 in the frequency band of interest (i.e., delta, theta, alpha, beta),  $bexp$  is the baseline-corrected (i.e.,  
369 sentence presentation – pre-sentence interval) exponent of the aperiodic  $1/f$  slope,  $type$  refers to  
370 Sentence Type (fixed, flexible),  $sag$  is Sagittality (anterior, central, posterior) and  $lat$  refers to Laterality  
371 (left, midline, right). Participant ID ( $participant$ ) was modelled as a random intercept.  $\epsilon$  refers to a  
372 Gaussian-distributed error term.

373 Type II Wald  $\chi^2$ -tests from the `car` package (Fox et al., 2011) were used to provide  $p$ -values.  
374 An 83% confidence interval (CI) threshold was adopted for visualisations, which corresponds to the

375 5% significance level with non-overlapping estimates (Austin & Hux, 2002; MacGregor-Fors &  
 376 Payton, 2013). General linear models were performed to assess the relationship between baseline  
 377 corrected oscillatory power and aperiodic  $1/f$  slope between fixed and flexible word orders. Baseline-  
 378 corrected oscillatory power values were  $\log_{10}$  transformed prior to model inclusion. All data, as well as  
 379 analysis scripts (MATLAB and R) are available on the OSF platform: <https://osf.io/7yr46/>; Cross,  
 380 Corcoran, Schlesewsky, Kohler, & Bornkessel-Schlesewsky, 2022). For a schematic visualisation of  
 381 EEG signal processing and statistical analysis steps, see Figure 2.



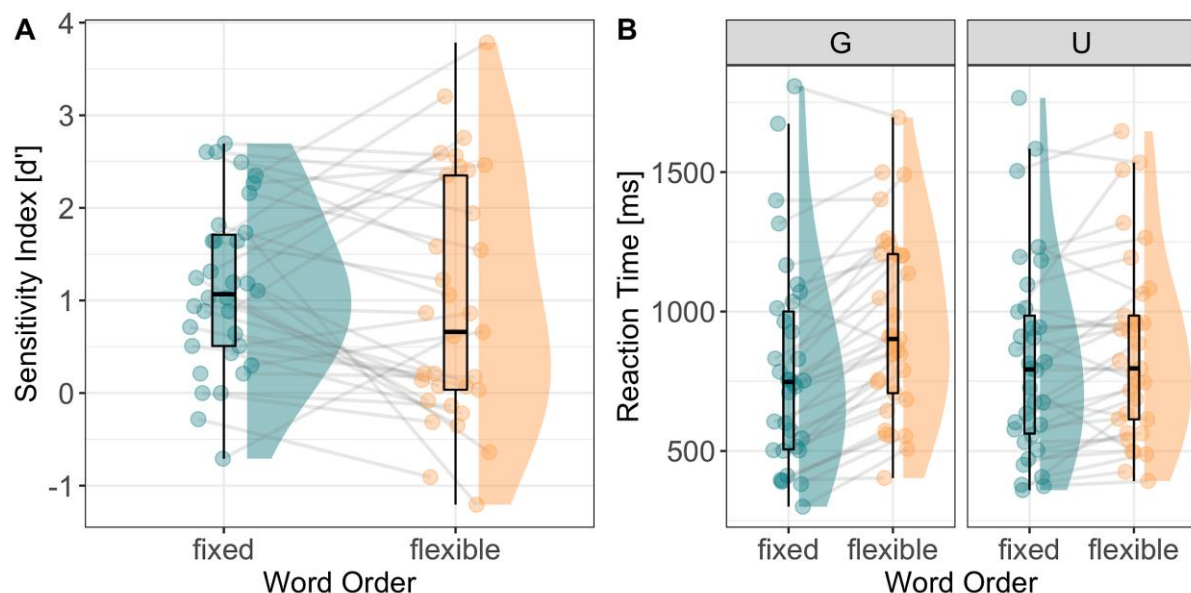
382 **Figure 2. Schematic of the EEG recording, pre-processing, signal, and statistical analysis**  
 383 **procedures.** a. Neurophysiological signals were recorded at rest and during the sentence learning task  
 384 using a 32-channel EEG system. b. The EEG signal was filtered, re-referenced and subjected to an  
 385 independent component analysis. c. The individual alpha frequency (IAF) was estimated per participant  
 386 from resting-state EEG recordings based on an occipital-parietal electrode cluster (see topoplott). Peak  
 387 frequencies within the alpha band (7-14 Hz; light blue shading) were identified using restingIAF, an  
 388 automated procedure that smoothes and differentiates the power spectrum before estimating the average  
 389 IAF (dotted line) across selected channels. IAF estimates were subsequently used to calculate  
 390 participant-specific delta, theta, alpha and beta centre frequencies ( $f_c$ ) and bandwidths ( $f_1$ ,  $f_2$ ) for the  
 391 time-frequency decomposition of the sentence learning task. d. (i) Grand-average time-frequency  
 392 representation of fixed word order sentences during the learning session. Dashed black boxes  
 393 correspond to the presentation of elements in the stimulus train above. (ii) Histograms illustrating the  
 394 distribution of the aperiodic exponent and alpha power estimated using FOOOF (pink) and IRASA  
 395 (blue). e. (i) Single-subject power spectral density (PSD) plots at the beginning (left) and end (right) of  
 396 the sentence learning task. Straight turquoise and tan lines represent the IRASA-based aperiodic  
 397 regression fit for fixed and flexible word order sentences, respectively. (ii) PSD plots illustrating power  
 398 in the IAF-derived delta ( $\delta$ ), theta ( $\theta$ ), alpha ( $\alpha$ ) and beta ( $\beta$ ) bands after subtraction of the aperiodic  
 399

400 regression fit depicted in (i). (iii) Raw data at electrode Cz illustrating the analysis performed to estimate  
401 time-varying modulations in the aperiodic exponent between fixed and flexible word orders. (iv)  
402 scatterplots illustrating the analyses predicting behaviour (i.e., judgement accuracy [ $d'$ ]) from the  
403 sentence judgement task from aperiodic and oscillatory activity derived from the sentence learning task.

404 **Results**

405 **Task performance**

406 The results on the judgement task are visualised in Figure 3. Participants performed moderately  
407 well on the judgement task, with a mean  $d'$  score of 1.02 (range: -1.20 – 3.78) and mean reaction time  
408 of 878.08 ms (range: 254.75 – 2076.83). There is clearly a high degree of inter-individual variability  
409 across both fixed and flexible sentences; however, flexible sentences had greater variability in  $d'$  scores,  
410 while fixed grammatical sentences had faster responses overall. For a detailed report and interpretation  
411 of these behavioural data, see Cross et al. (2020a).



412

413 **Figure 3.** Raincloud plots illustrating the behavioural responses during the sentence judgement task.  
414 (A) Mean  $d'$  scores (x-axis) for Fixed and Flexible sentence types. (B) Mean reaction time (ms; x-axis)  
415 for Grammatical (left) and Ungrammatical (right) Fixed and Flexible sentence types. Individual data  
416 points represent the mean for each participant, while the lines join within-participant differences  
417 between fixed and flexible word order sentences.

418

419 **Neurophysiological results**

420 Individual alpha frequency estimates varied between participants ( $M_{IAF} = 9.78$ ,  $SD = 0.96$ ),  
421 resulting in a range of participant-specific frequency bands (summarised in Table 1). A full list of  
422 participant-specific IAFs and frequency bandwidth are available on the OSF repository.

423 **Table 1.** Mean lower ( $f_1$ ) and upper ( $f_2$ ) frequency bounds for the delta, theta, alpha and beta bands.  
424 Participant-specific range provides the lowest and highest frequency band limits based on single-  
425 participant estimates, as is also provided for IAF estimates.

Band	Mean $f_1$ (SD)	Mean $f_2$ (SD)	Participant-Specific Range
Delta	1.83 (0.18)	3.67 (0.36)	1.42 – 4.33
Theta	3.67 (0.36)	7.34 (0.72)	2.83 – 8.66
Alpha	7.34 (0.72)	14.7 (1.45)	5.67 – 17.33
Beta	14.7 (1.45)	29.4 (2.90)	11.36 – 34.67
IAF	--	--	7.57 – 11.55

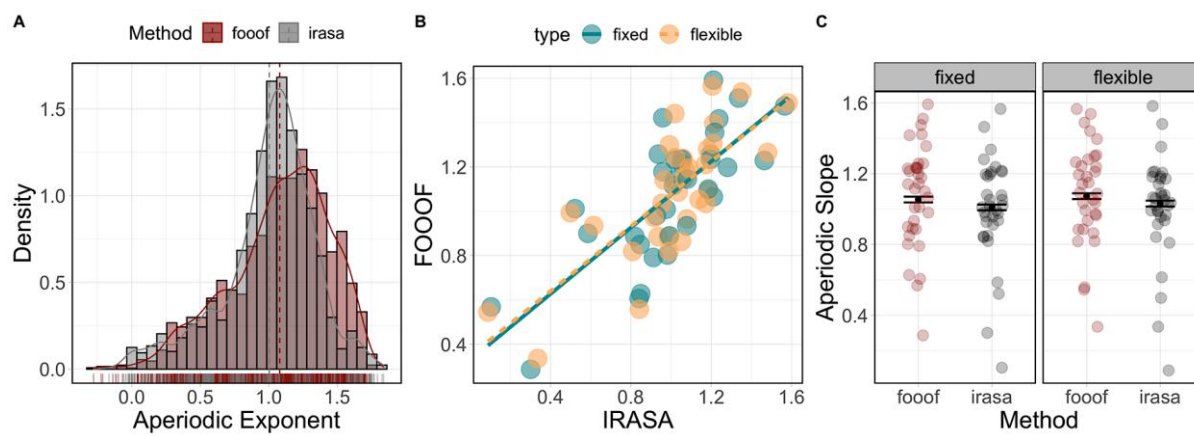
426  
427 *Note.* SD = standard deviation; IAF = individual alpha frequency. Participant-specific range provides  
428 the absolute lowest and upper band limits.

429  
430 *Aperiodic and oscillatory changes across time and space during language learning*

431 Neurophysiological signals are non-stationary, showing dynamic changes over time as a  
432 function of endogenous and exogenous factors (e.g., Donoghue, Schaworonkow & Voytek, 2021), such  
433 as attentional fluctuations and the complexity of incoming sensory information (Waschke et al., 2021).  
434 However, neurophysiological signals are typically analysed using linear models, which often do not  
435 capture non-linear modulations in neural activity, particularly over time. Here, we examine how  
436 aperiodic and oscillatory dynamics evolve over time during language learning, focusing specifically on  
437 the way in which spectral activity varies across sentence types (fixed vs flexible word orders). Estimated  
438 changes in aperiodic and oscillatory spectral activity across learning task conditions are illustrated in  
439 Figure 5 (for topographical maps, see Figure 6).

440 Comparisons between IRASA and FOOOF showed that FOOOF provided higher exponent  
441 estimates than IRASA, irrespective of sentence type (fixed, flexible; Figure 4) and were also more  
442 variable ( $M_{FOOOF} = 1.08$ ,  $SD = 0.48$ ;  $M_{IRASA} = 1.00$ ,  $SD = 0.42$ ). However, exponent estimates between  
443 IRASA and FOOOF were highly positively correlated across both fixed ( $\rho = 0.75$ ,  $p < .001$ , 83% CI =  
444 [.63, .84] and flexible ( $\rho = 0.76$ ,  $p < .001$ , 83% CI = [.63, .85]; Figure 4B) word order sentences. These  
445 observations were complemented by a linear mixed-effects regression which revealed that while

446 FOOOF had overall higher exponent estimates than IRASA ( $\beta = 0.02$ ,  $se = 0.004$ ,  $p < .001$ ), exponent  
447 estimates between FOOOF and IRASA did not vary by sentence type ( $\beta = 0.0005$ ,  $se = 0.004$ ,  $p = .89$ ;  
448 Figure 4C). These observations are consistent with simulations reported by Donoghue et al., 2020;  
449 however, given that there was no significant interaction between method (FOOOF, IRASA) and  
450 sentence type (fixed, flexible), we present the IRASA-based analysis.



451  
452 **Figure 4.** Comparison between FOOOF and IRASA exponent estimates. (A) Histogram illustrating the  
453 distribution of exponent estimates derived from FOOOF (red) and IRASA (grey). (B) Scatterplot  
454 showing the relationship between FOOOF (y-axis) and IRASA (x-axis) between fixed (turquoise) and  
455 flexible (tan) sentences. (C) Relationship between the aperiodic exponent (y-axis; higher values indicate  
456 a steeper exponent), method (x-axis; FOOOF, IRASA), and sentence type (left facet = fixed, right facet  
457 = flexible). Bars represent the 83% confidence interval around group-level expected marginal mean  
458 estimates. Dots represent individual data points per participant for aggregated data.

459  
460 The  $\chi$ -exponent GAMM revealed the  $1/f$  slope was steeper on average for Flexible compared  
461 to Fixed word order sentences ( $\beta = 0.02$ ,  $SE = 0.008$ ,  $F(1) = 5.84$ ,  $p = .015$ ). Visualisation of smooth  
462 terms (Figure 5A) revealed that exponent values tended to decrease (indicating a flattening of the  $1/f$   
463 slope) over the course of the learning period; however, Flexible trials evoked higher values (steeper  $1/f$   
464 slopes) at the beginning and during the second half of the session, relative to Fixed trials (Trial  $\times$   
465 Sentence Type estimated degrees of freedom [ $edf$ ] = 3.87,  $F = 29.67$ ,  $p < .001$ ). This model further  
466 revealed significant topographic differences between conditions, with Flexible word orders evoking  
467 higher exponent values over fronto-central regions compared to Fixed word order sentences by the end  
468 of the session (Trial  $\times$  Sagittality  $\times$  Sentence Type  $edf = 1.78$ ,  $F = 1.13$ ,  $p < .001$ ; see Figure 6; for full  
469 summary tables of all models, see Appendix).

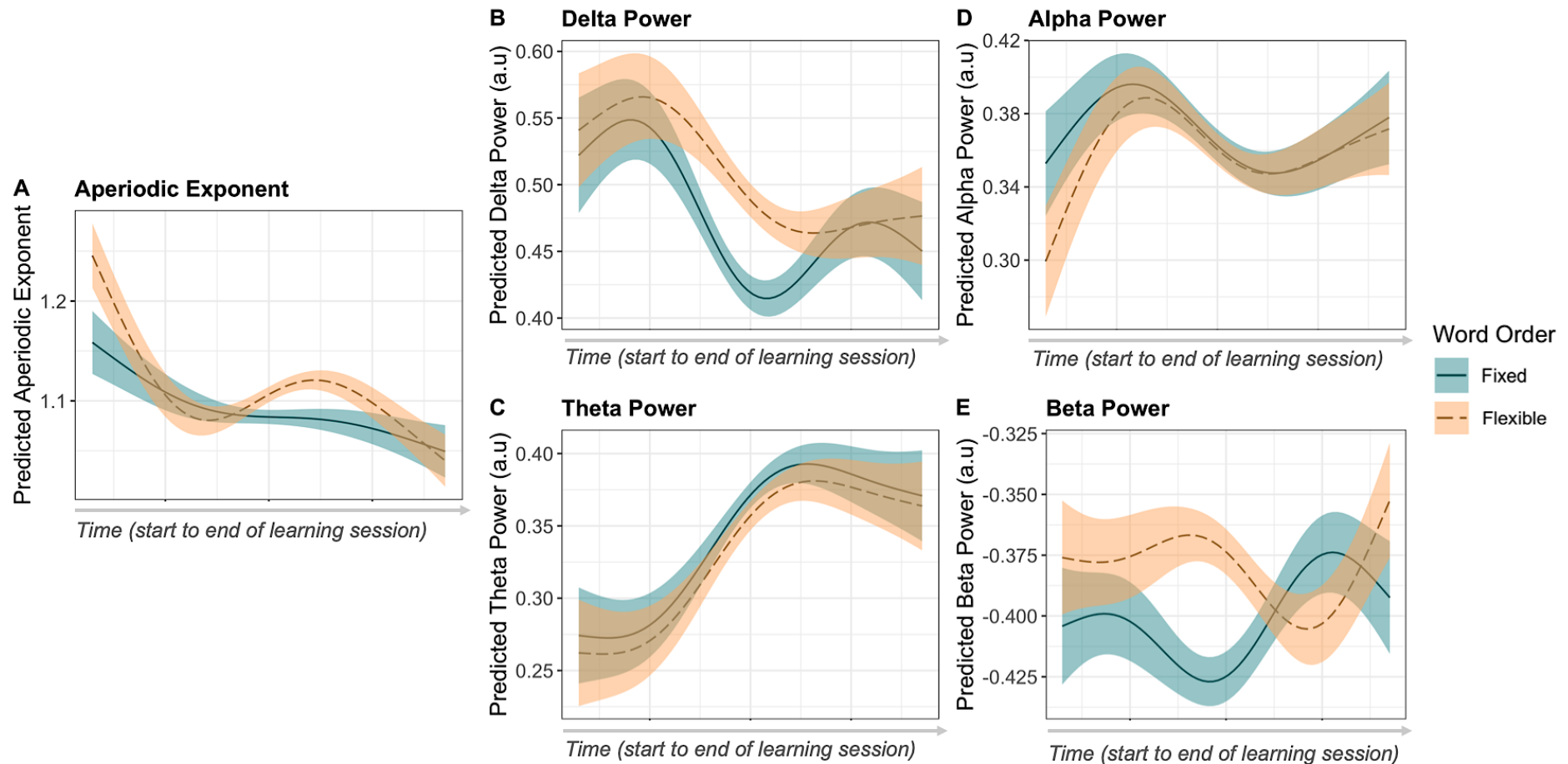
470 Mean delta power was higher on average during Flexible compared to Fixed word order trials,  
471 although this difference was not significant ( $\beta = 0.03$ ,  $SE = 0.016$ ,  $F = 3.68$ ,  $p = .055$ ). However,

472 visualisation of smooth terms (Figure 5B) revealed a complex pattern whereby delta power increased  
473 over early trials, followed by a marked decrease that was more pronounced in response to Fixed than  
474 Flexible sentence stimuli ( $edf = 2.74, F = 9.66, p < .001$ ). This interaction was significantly modulated  
475 by sagittality, with between-condition differences (Fixed versus Flexible) in mean power density  
476 increasing over fronto-central electrodes as a function of time ( $edf = 2.68, F = 1.54, p < .001$ ). Theta  
477 power was non-significantly lower on average during Flexible compared to Fixed rule learning ( $\beta = -$   
478  $0.01, SE = 0.014, F = 0.60, p = .437$ ). Again, smooth terms revealed a nonlinear pattern of spectral  
479 fluctuation, whereby theta power evinced a sigmoidal shape over the course of rule-learning (Figure  
480 5C). This pattern was similar across both conditions, with Fixed sentence stimuli tending to evoke  
481 increased theta power ( $edf = 0.824, F = 1.25, p = .014$ ). This pattern of activity varied as a function of  
482 topography, with the difference between conditions being more accentuated across lateralised and  
483 posterior sites, as illustrated in Figure 6 ( $edf = 7.63, F = 0.22, p = .003$ ).

484 Alpha power tended to increase over the early and later trials of the learning task, although this  
485 pattern was interrupted by a marked decline during the middle of the session ( $edf = 3.20, F = 12.50, p$   
486  $< .001$ ). Flexible word orders evoked less alpha power than Fixed word orders at the beginning of the  
487 session, but was similar thereafter ( $edf = 3.20, F = 13.46, p < .001$ ; Figure 5D). This difference was  
488 most pronounced over left-lateralised and frontal sites ( $edf = 2.27, F = 0.35, p = .012$ ). Finally, the beta  
489 power model revealed significant differences in the nonlinear profile of power dynamics across the  
490 learning session. In fact, Fixed and Flexible trials evoked markedly different patterns of activity: beta  
491 power showed an approximately triphasic response to Fixed sentence stimuli that was mirrored by the  
492 response to Flexible stimuli ( $edf = 2.94, F = 30.08, p < .001$ ; Figure 5E). The strongest beta response  
493 was observed over frontal and temporal regions ( $edf = 16.59, F = 33.04, p < .001$ ), particularly toward  
494 the beginning of the learning phase for Flexible word order sentences ( $edf = 6.82, F = 1.24, p < .001$ ).

495 Taken together, these data illustrate dynamic changes in both aperiodic and oscillatory activity  
496 as a function of different word order rules during learning. Both the aperiodic slope and delta power  
497 tended to decrease over time, while theta power tended to increase. By contrast, alpha and especially  
498 beta power evinced more complex dynamics as participants learnt different word order rules.

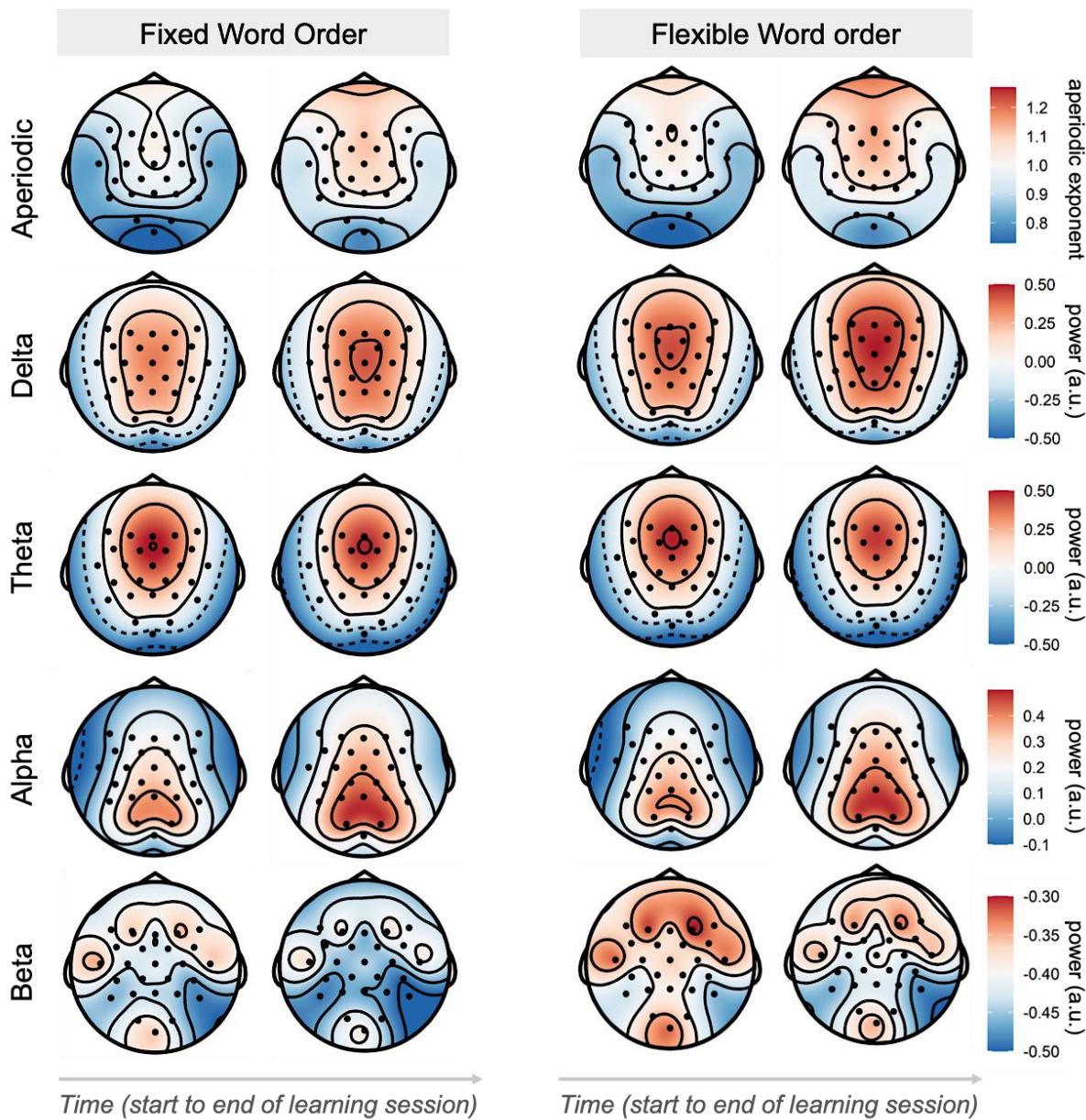
499



500

501 **Figure 5.** Modelled effects for changes in the aperiodic exponent (A), delta (B), theta (C), alpha (D) and beta (E) activity across the learning task for fixed  
 502 flexible (dashed line) word order rules. Time from beginning to the end of the learning task is represented on the x-axis.

503



504

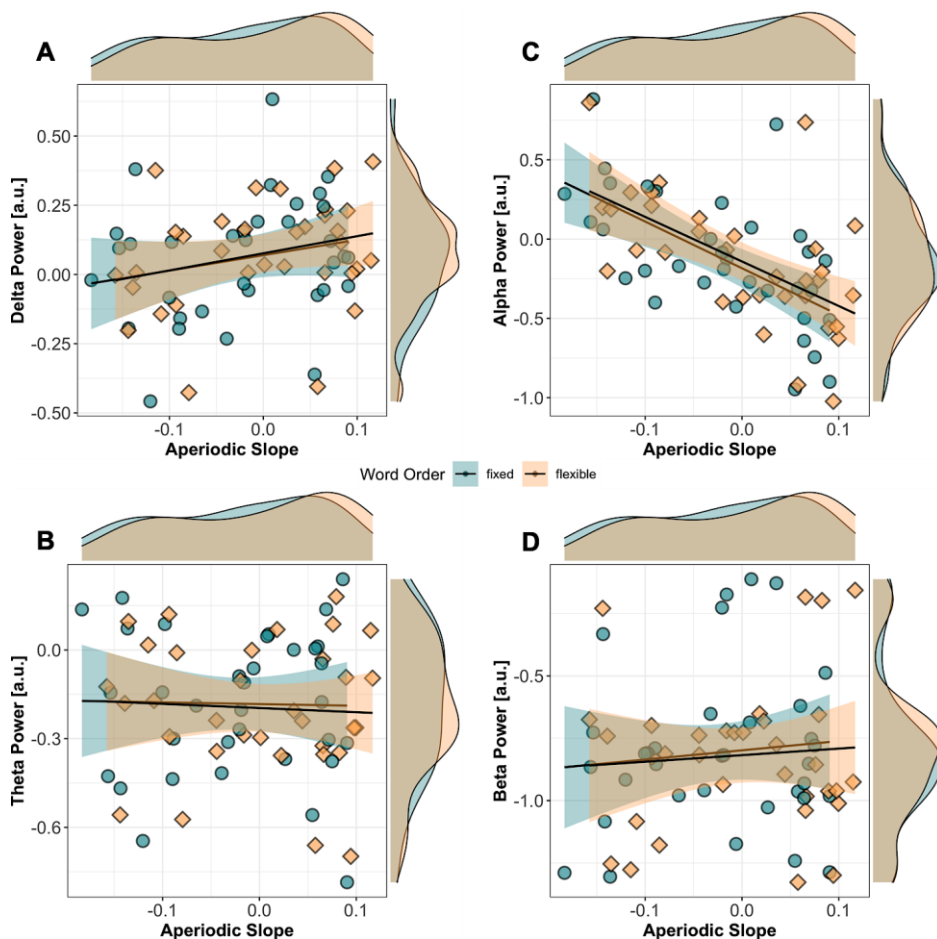
505 **Figure 6.** Difference in topographical distribution of aperiodic and oscillatory activity between fixed  
506 and flexible word order sentences at the beginning and end of the sentence learning task.

507

508 *Task-related aperiodic and oscillatory activity are dynamically related during language learning*

509       Neurophysiological signals are dominated by transient oscillatory and broadband aperiodic  
510 activity; however, in the study of the oscillatory correlates of higher-order language processing,  
511 aperiodic activity is rarely considered, with little known regarding its influence on task-related  
512 oscillatory activity (cf. Cross et al., 2021). Here, we examined the associations between task-related  
513 oscillations in individualised (i.e., anchored on participants' IAF) frequency bands and aperiodic  
514 activity during the learning of different word order rules. There was non-significant positive association

515 between delta power and the aperiodic slope ( $\beta = 0.58, p = .05, R^2 = 0.02$ ). There was no relationship  
516 between theta power and the aperiodic slope ( $\beta = 0.09, p = .77, R^2 = -0.04$ ); however, there was a  
517 significant negative association between alpha power and the aperiodic slope ( $\beta = -2.88, p < .001$ ,  
518  $R^2 = 0.33$ ), which did not vary by sentence type. Finally, there was no significant relationship between  
519 task-evoked beta power and the aperiodic slope ( $\beta = 0.31, p = .49, R^2 = -0.04$ ; for a visualisation of these  
520 associations, see Figure 7). These results indicate that aperiodic and narrowband spectral estimates may  
521 afford complementary information about learning and task performance. Based on this, we now  
522 examine whether such aperiodic and (putative) oscillatory activity interact to predict performance on  
523 the sentence judgement task.



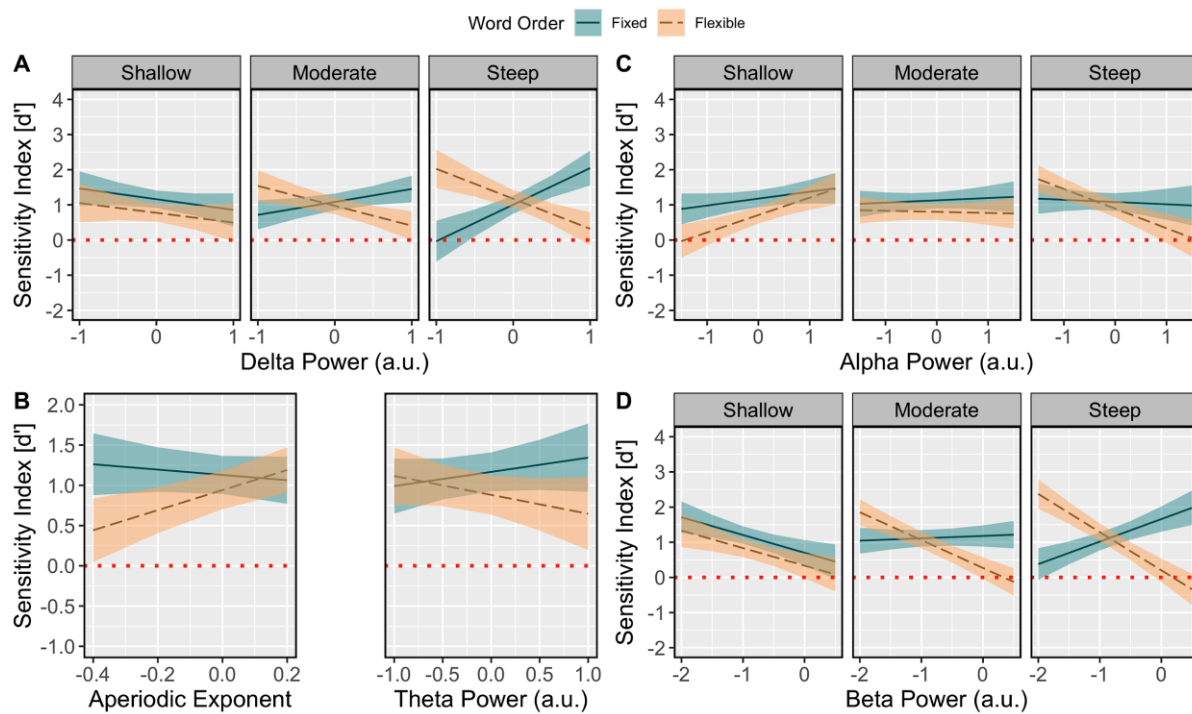
524  
525 **Figure 7.** Association between task-related aperiodic slope and oscillatory power in the delta (A), theta  
526 (B), alpha (C) and beta (D) bands during the sentence learning task averaged across all channels. The  
527 aperiodic slope is represented on the x-axis (higher values indicate a steeper slope relative to the pre-  
528 sentence interval), while oscillatory power is represented on the y-axis (higher values indicate higher  
529 power relative to the pre-sentence interval). The density of observations for frequency band power and  
530 the aperiodic slope are indicated on the margins of each plot, while the fixed and flexible word order  
531 sentences are coded in turquoise and tan, respectively.

532 *Interactions between oscillatory and aperiodic activity modulate behavioural performance*

533 Given the association between task-related oscillatory and aperiodic activity during the learning  
534 of complex linguistic rules, we now examine whether the  $1/f$  slope and oscillatory activity interact  
535 during learning to influence behavioural performance on the sentence judgement task. For all analyses,  
536 we used linear mixed-effects regression models (for full summary tables for all models, see Appendix).  
537 For the delta model, there was a significant Power  $\times$   $1/f$  Slope  $\times$  Sentence Type interaction ( $\chi^2(1) =$   
538 12.47,  $p < .001$ ). As shown in Figure 8A, when the  $1/f$  slope was steepest and delta power was low,  $d'$   
539 was higher for flexible relative to fixed word orders. By contrast, when the  $1/f$  slope was steep and  
540 delta power was high, performance for fixed word orders increased. For the theta model, there was a  
541 significant Power  $\times$  Sentence Type ( $\chi^2(1) = 4.57, p = .03$ ) and  $1/f$  Slope  $\times$  Sentence Type interaction  
542 ( $\chi^2(1) = 17.43, p < .001$ ). Here, when the  $1/f$  slope was steep,  $d'$  scores increased for flexible sentences  
543 (Figure 8B; left). By contrast, when theta power increased, performance for both fixed sentences was  
544 higher (Figure 8B; right).

545 For the alpha model, there was a significant three-way Power  $\times$   $1/f$  Slope  $\times$  Sentence Type  
546 interaction ( $\chi^2(1) = 15.94, p < .001$ ). As depicted in Figure 8C, when the  $1/f$  slope was shallow, and as  
547 alpha power increased,  $d'$  scores were higher for both fixed and flexible word orders. By contrast, when  
548 the  $1/f$  slope was steep, and as alpha power decreased,  $d'$  scores were lower for flexible word order  
549 sentences. Similarly, the beta model yielded a significant Power  $\times$   $1/f$  Slope  $\times$  Sentence Type  
550 interaction ( $\chi^2(1) = 30.96, p < .001$ ). When the  $1/f$  slope was shallow, and as beta power decreased,  $d'$   
551 scores were higher for both fixed and flexible word orders (Figure 8D). By contrast, when the  $1/f$  slope  
552 was steep, increased beta power predicted higher  $d'$  scores for fixed but lower  $d'$  scores for flexible  
553 word order sentences, respectively.

554 Together, these results suggest that when there is a steeper  $1/f$  slope, increased delta and beta  
555 power were associated with better behavioural performance, and thus better learning outcomes for fixed  
556 relative to flexible word order sentences. Further, when the  $1/f$  slope was shallow and alpha power  
557 decreased, there was a general benefit in performance for both fixed and flexible word order sentences,  
558 relative to when the  $1/f$  slope was steep.



559 **Figure 8.** Visualisation of the relation between behavioural performance, aperiodic slope, and  
 560 oscillatory delta (A), theta (B), alpha (C), and beta (D) activity. Modelled effects of task-related  
 561 oscillatory activity (x-axis; higher values indicate greater power) on  $d'$  scores (y-axis; higher values  
 562 indicate better performance) for fixed and flexible word order sentences (fixed = solid line; flexible =  
 563 dashed line). Task-related aperiodic  $1/f$  slope estimates are faceted from shallow (left), to moderate  
 564 (middle), to steep (right). Note that the trichotomisation of the aperiodic slope into shallow, moderate  
 565 and steep facets is for visualisation purposes only, with the aperiodic slope being entered into all models  
 566 as a continuous predictor. Note that (B) illustrates the two-way modelled interaction effects of task-  
 567 related aperiodic slope (left; x-axis, higher values indicate a steeper slope) and theta power (right; x-  
 568 axis, higher values indicate greater power) for fixed and flexible word order sentences (fixed = solid  
 569 line; flexible = dashed line). The red dashed line indicates chance-level performance, while the shaded  
 570 regions indicate the 83% confidence interval. For A, B, C and E, the x-axis reflects scaled single-trial  
 571 oscillatory power estimates, with negative values reflecting a decrease in power and positive values  
 572 reflecting an increase in power.

573  
 574  
 575 **Discussion**  
 576 Here, we estimated the  $1/f$  slope during artificial grammar learning to characterise the influence  
 577 of dynamic alterations in aperiodic and oscillatory activity on higher-order cognition. This is the first  
 578 study to examine aperiodic activity and its interaction with oscillatory power in the context of language  
 579 learning, with three critical findings emerging: (1) both (putative) oscillatory and aperiodic activity  
 580 dynamically change over time during complex language-related rule learning; (2) the  $1/f$  slope becomes  
 581 steeper during the learning of complex rules, but this effect differed depending on the type of rules  
 582 being learned, and; (3) learning-related aperiodic activity interacted with oscillatory power to modulate

583 behavioural performance for both fixed and flexible word orders. These findings speak strongly to the  
584 view that aperiodic  $1/f$  dynamics should be explicitly modelled or isolated as a source of variance when  
585 analysing power spectra to ensure that any oscillatory changes are not confounded with modulations in  
586 broadband aperiodic activity (Donoghue et al., 2021).

587 Indeed, a considerable proportion of work examining the oscillatory correlates of higher-order  
588 language processing have not explicitly accounted for modulations in broadband aperiodic activity (e.g.,  
589 Bonhage et al., 2017; Corcoran et al., 2022; Kepinska et al., 2017; Lewis et al., 2016; Mai, Minett, &  
590 Wang, 2016; Prat et al., 2016; Rossi & Prystauka, 2020; c.f., Cao et al., 2022), making it difficult to  
591 determine whether oscillatory activity parsimoniously explains behavioural outcomes. By separating  
592 oscillatory and aperiodic components, we have demonstrated that the aperiodic exponent flattens across  
593 time, while, for example, theta and alpha power increase across time throughout the language learning  
594 phase. Recent computational work has highlighted the criticality of such a separation of neural signals  
595 (e.g., Donoghue et al., 2020), given that both aperiodic and oscillatory signals vary by clinical status  
596 (Robertson et al., 2019), state of consciousness (e.g., sleep versus wake; Lendner et al., 2020), and are  
597 modulated by task demands (Waschke et al., 2021). From this perspective, language studies reporting  
598 differences in oscillatory activity (e.g., increases in theta power) between experimental conditions (e.g.,  
599 grammatical vs ungrammatical sentences) without accounting for broadband activity may be  
600 confounded by changes in aperiodic dynamics (Donoghue et al., 2021).

### 601 **Aperiodic and oscillatory activity are modulated by time-on-task**

602 The potential confounding of aperiodic and oscillatory components is further compounded by  
603 the fact that neural activity is non-stationary (Donoghue et al., 2021; Kosciessa et al., 2020; Stokes &  
604 Spaak, 2016). Here, we modelled single trial fluctuations of both aperiodic and oscillatory EEG  
605 components across the learning task, revealing fine-grained temporal dynamics underlying complex  
606 rule learning. For the aperiodic component, we observed a general flattening of the slope across time  
607 for both fixed and flexible sentences; however, the slope was steeper overall for flexible sentences. The  
608 general flattening of the aperiodic slope across time is in line with previous work reporting attentional  
609 modulations of spectral exponents (Kosciessa et al., 2021; Waschke et al., 2021). As exposure to  
610 grammar rules increased with time-on-task, participants may have become more adept at allocating

611 attention to cues relevant for successful sentence interpretation. Increased attentional modulation in  
612 accordance with learnt rules may have been accompanied by increased excitation/inhibition ratio, which  
613 reflects an increase in high-frequency power in cortical regions involved in processing task-relevant  
614 information (Cohen & Maunsell, 2011; Harris & Thiele, 2011), thus explaining the flattening of the  
615 aperiodic slope (Kosciessa et al., 2021; Waschke et al., 2021).

616 The observed increases in theta and alpha power over time are also consistent with previous  
617 work on complex rule and language learning (e.g., Crivelli-Decker et al., 2018; de Diego-Balaguer,  
618 Fuentemilla, & Rodriguez-Fornells, 2011; Kepinska et al., 2017). In the few studies examining the  
619 neural oscillations involved in grammar learning (e.g., de Diego-Balaguer et al., 2011; Kepinska et al.,  
620 2017), it has been demonstrated that theta and alpha synchronisation predict learning success. Here,  
621 theta and alpha power showed a non-linear increase in power across the learning task. Theta oscillations,  
622 particularly over frontal regions when recorded with scalp-EEG, are associated with plasticity-related  
623 learning and memory processes, reflecting the encoding and generalisation of new information  
624 (Eschmann et al., 2020; Khader et al., 2010). From this perspective, the observed increase in theta power  
625 for both fixed and flexible word orders may have reflected successful memory encoding and  
626 accumulating knowledge of the underlying grammatical rules.

627 Beta activity also displayed complex non-linear changes for fixed and flexible word orders  
628 across the learning task. Overall, beta power was higher for flexible than fixed word orders, particularly  
629 in the second half of the learning session (Figure 5E). In the native language processing literature  
630 (Bastiaansen et al., 2010; Davidson & Indefrey, 2007; Kielar et al., 2014, 2015), beta oscillations are  
631 argued to reflect prediction-related activity, with beta power increasing in highly predictable linguistic  
632 contexts, and decreasing when grammatical violations occur (for review, see Lewis et al., 2015, 2016).  
633 However, in studies on second language learning (e.g., Lewis et al. 2016), beta power increases in  
634 response to sentences with long-distance dependencies, possibly indicating more effortful processing  
635 (Meyer et al., 2013). From this position, the observed general increase in beta power for both fixed and  
636 flexible word orders across the task may reflect the accumulation of grammatical knowledge, allowing  
637 participants to better predict underlying rules of the language. Further, the marked increase in beta  
638 power for flexible word order processing may indicate more effortful processing, given that flexible

639 word orders contain non-adjacent elements that require integration for successful comprehension (Cross  
640 et al., 2018).

641 **Interactions between aperiodic and oscillatory activity predict learning**

642 Interactions between oscillatory and aperiodic activity during the learning task also predicted  
643 subsequent behavioural performance. Increased alpha power predicted an increase in performance for  
644 fixed word orders when the aperiodic  $1/f$  was shallow, while a decrease in alpha power predicted higher  
645 performance for flexible word orders when the aperiodic slope was steep. By contrast, when the  
646 aperiodic slope was shallow, a decrease in beta power (i.e., beta desynchronisation) was associated with  
647 improved behavioural performance for both fixed and flexible word orders. Further, when the aperiodic  
648 slope was steep, the relationship between beta desynchronisation and flexible word order processing  
649 was stronger, but the inverse was observed for fixed word order sentences.

650 The effect of differing levels of  $1/f$  slope on, for instance, beta power and behavioural  
651 performance likely reflect more nuanced inter-individual differences in information processing  
652 capacities (Dziego et al., 2022; Immink, Cross et al., 2021; Thuwal, Banerjee, & Roy, 2021), which  
653 may explain behavioural gains that are otherwise related to the manifestation of oscillatory activity  
654 (e.g., Kepinska et al., 2017). For example, here we observed that a decrease in beta power predicted  
655 better behavioural performance for flexible rules, while the inverse was seen for fixed word order rules.  
656 From this perspective, a steeper slope may be more conducive for learning more complex information  
657 based on distinct neural dynamics, reflecting a decrease in the excitation/inhibition balance, and thus a  
658 decrease in high-frequency activity (Cohen & Maunsell, 2011; Harris & Thiele, 2011; Waschke et al.,  
659 2021). A reduction in high-frequency activity has been associated with error-driven learning (Luft,  
660 Takase, & Bhattacharya, 2014; Luft, 2014; Tan, Jenkinson, & Brown, 2014) and predictive processing-  
661 based activity (Bastos et al., 2012; Arnal & Giraud, 2012), particularly in the context of language  
662 comprehension (Cross et al., 2018; Lewis & Bastiaansen, 2015; Lewis et al., 2016). As such, a steeper  
663  $1/f$  slope, which was observed for flexible relative to fixed word order rules across the learning task  
664 (Figure 5A), may be foundational for task-related oscillatory activity during higher-order language  
665 learning.

666 The oscillatory-based findings are also broadly consistent with previous work (e.g., Kepinska  
667 et al., 2017), but reveal fine-grained patterns of spectral activity between word order variations, which  
668 may be explained by cue-integration-based models of language processing (Bates et al., 2001;  
669 Bornkessel & Schlesewsky, 2006; Bornkessel-Schlesewsky et al., 2015; Kaufeld et al., 2020; Martin,  
670 2016). Under this framework, cues that are differentially weighted according to the probabilities of the  
671 language are integrated to comprehend incoming linguistic input (e.g., sentences). Here, fixed word  
672 orders contained linear order-based cues, which are analogous to English, while flexible word orders  
673 required animacy-based cues for interpretation. From this perspective, and in line with previous work  
674 on sequence processing (Crivelli-Decker et al., 2018; Kikuchi, et al., 2018; Wang et al., 2019), increased  
675 beta power likely reflected the propagation of top-down predictions during the learning of fixed word  
676 orders (Cross et al., 2018). In fixed sentences, the first noun is invariably the Actor, and as such,  
677 predictions are constrained to anticipating that the second noun will be the Undergoer, while also  
678 containing a verb-final construction. Therefore, due to the strong sequence dependence in fixed word  
679 orders, precision-weighted predictions would likely increase linearly across the sentence, manifesting  
680 in increased beta power (Arnal, 2012; Cross et al., 2018; Lewis & Bastiaansen, 2015).

681 The inverse relationship with flexible word order processing – which was predicted by a  
682 reduction in beta power – can also be explained under this framework. Given that flexible word orders  
683 contain either Actor-first or Undergoer-first constructions, predictions cannot be based on the linear  
684 position of the words, and instead must be driven by the integration of (non-adjacent) animacy-based  
685 cues to arrive at an accurate sentential percept. Given that our sample consisted of native monolingual  
686 English speakers (a language that relies heavily on word order cues; Bates et al., 2001; Bornkessel-  
687 Schlesewsky, et al. 2011; MacWhinney et al., 1984), a reduction in beta power during flexible word  
688 order processing likely reflected prediction errors and internal model updating. That is, beta  
689 desynchronization during the learning of flexible word orders may have reflected internal model  
690 updating based on mismatches with predicted and actual sensory input, while an increase in beta power  
691 during fixed word order processing likely reflected the accumulation of top-down predictions based on  
692 our sample of native English speakers' preference for word-order-based cues. Importantly, this  
693 interpretation is consistent with temporal sequence learning paradigms, where beta power increases for

694 fixed relative to “random” sequences (Crivelli-Decker et al., 2018), which also aligns with the observed  
695 beta power increase from the second half the learning task for fixed relative to flexible word orders  
696 (Figure 5E).

697 Alpha activity showed a similar interaction: when the  $1/f$  slope was steep, reduced alpha power  
698 (i.e., alpha desynchronisation) predicted flexible word order processing. Alpha power reductions during  
699 language comprehension may reflect goal-directed processing and enhanced allocation of attentional  
700 resources, which is required for the successful learning of flexible word orders (Kepinska et al., 2017),  
701 given that they deviate from the canonical English word order (Bates et al., 2001). This interpretation  
702 is in line with evidence demonstrating that alpha oscillations reflect rhythmic cortical gating by  
703 alternating the activation of task-relevant cortical regions while inhibiting the processing of task-  
704 irrelevant information (Chapeton et al., 2019; de Vries et al., 2020; Gallotto et al., 2020; Klimesch,  
705 2012; Jensen & Mazaheri, 2010). From this perspective, a decrease in alpha power likely facilitated the  
706 extraction of flexible word order rules by suppressing task-irrelevant input and optimising cortical  
707 communication in a selectively precise manner, promoting the encoding and consolidation of non-  
708 canonical grammatical rules. This interpretation is also supported by the observation that alpha power  
709 was lower for flexible relative to fixed word order rules, particularly at the beginning of the learning  
710 task (Figure 5D).

711 We also found that an increase in theta power predicted performance for flexible but not fixed  
712 word orders; however, theta did not interact with the aperiodic exponent to predict behavioural  
713 performance. Theta oscillations have been proposed to combine linguistic input into successively more  
714 complex representations, establishing relations between (non-adjacent) elements in a sentence  
715 (Covington & Duff, 2016; Cross et al., 2018). The positive association between theta power and  
716 performance for flexible word orders may reflect the learning and integration of non-adjacent rules,  
717 which involves the decoding and combination of words that are non-adjacent in a sentence. Indeed,  
718 such theta effects have been reported during native sentence processing (Lam et al., 2016). These effects  
719 are also consistent with the general memory literature: retrieval of language (e.g., single words), and  
720 shape/face stimuli elicit higher theta synchronisation (Bastiaansen et al., 2002; Klimesch et al., 2008;  
721 Klimesch et al., 2010; Mormann et al., 2005; Osipova et al., 2006), with these effects manifesting over

722 medial temporal and prefrontal cortices (Guderian & Düzel, 2005), indexing the activation of relevant  
723 memory traces and executive control processes, respectively.

724 **Functional relevance of aperiodic activity in language and higher-order cognition**

725 Our analysis revealed a link between aperiodic activity during language learning and  
726 performance on a grammaticality judgement task. This finding is consistent with previous studies  
727 demonstrating the influence of aperiodic activity on a range of cognitive computations, including  
728 processing speed (Ouyang et al., 2020), memory (Sheehan et al., 2018) and prediction in language  
729 (Dave et al., 2018). From a neurophysiological perspective,  $1/f$ -like neural activity has been proposed  
730 to encode information relating to intrinsic brain function (Muthukumaraswamy & Liley, 2018),  
731 including the balance between excitation/inhibition (Gao et al., 2017), likely reflecting glutamate and  
732 GABA synaptic inputs into inter- and intra-cortical networks (Dave et al., 2018; Gao et al., 2017). Based  
733 on this perspective, Dave et al. (2018) argued that aperiodic activity influences prediction in language  
734 by modulating the strength of predictions of upcoming linguistic information via population spiking  
735 synchrony (Engel et al., 2001). This interpretation applies to our finding that aperiodic and beta activity  
736 showed a negative association with performance for fixed and flexible word orders: an increase in beta  
737 power predicted more sensitive behavioural responses for fixed sentences, while reduced beta predicted  
738 performance for flexible word orders. These findings can be explained by integrating two perspectives:  
739 the “spectral fingerprints” hypothesis (Hanslmayr & Staudigl, 2014; Keitel & Gross, 2016; Siegel et  
740 al., 2012; Watrous et al., 2015; Womelsdorf et al., 2014) and generalised predictive coding (Friston,  
741 2010, 2018, 2019).

742 The “spectral fingerprints” hypothesis argues that power changes in different frequency bands  
743 reflect distinct stages of memory and information processing (Fellner et al., 2019; Keitel & Gross,  
744 2016), rather than reflecting a “spectral tilt” between lower and higher frequencies. For example,  
745 decreases in alpha/beta and increases in gamma power during memory retrieval occur on different  
746 temporal scales and in different brain areas, providing evidence against proposals that a change in the  
747 tilt of the power spectrum solely drives memory computations (Fellner et al., 2019). Further, increases  
748 in high frequency gamma activity have been proposed to reflect the propagation of bottom-up sensory  
749 signals (Lewis et al., 2015; Richter, Thompson, Bosman, & Fries, 2017), while a decrease in alpha/beta

750 power is thought to index prediction errors (Bressler & Richter, 2015; Friston, 2019; Samaha, Bauer,  
751 Cimaroli, & Postle, 2015). From this perspective, a steeper  $1/f$  slope may reflect the maintenance of  
752 top-down predictions that allow comprehenders to generate expectations for incoming stimuli, thus  
753 minimizing prediction error at lower levels of the cortical hierarchy. This interpretation also holds for  
754 interactions observed with aperiodic and oscillatory activity in the alpha and beta bands, and as such,  
755 provides evidence that  $1/f$ -like activity may partially reflect cortical excitability across the frequency  
756 spectrum that serves to minimize prediction error during language learning and sentence processing.

757 **Conclusions and Future Directions**

758 Taken together, we have demonstrated that oscillatory and aperiodic activity jointly predict the  
759 learning of higher-order language. There are, of course, several open questions that arise from these  
760 results. For example, how do interactions between oscillatory and aperiodic activity relate to individual  
761 differences in atypical populations, such as those with schizophrenia and age-related pathologies,  
762 including Alzheimer's disease? Previous research has shown that cognitive deficits characteristic of  
763 schizophrenia may be better explained by changes in the  $1/f$  slope than irregularities in the canonical  
764 frequency bands (Peterson et al., 2018), and that  $1/f$  activity mediates age-related deficits in working  
765 memory (Voytek et al., 2015); however, the interaction between aperiodic and oscillatory activity  
766 during more complex cognitive computations, such as sequence learning and language processing,  
767 remains less well known. While we attempt to address the relationship between aperiodic and  
768 oscillatory activity during higher-order language learning, future work would benefit from examining  
769 how and if these interactions emerge in (age-related) pathologies, and whether patterns of aperiodic and  
770 oscillatory activity during language learning and sentence processing are generated by specific  
771 neuroanatomical networks. Such work will provide a better understanding of the neurobiology of  
772 cognition in both health and disease.

773

774

775

776

777

778

## References

779 Allen, M., Poggiali, D., Whitaker, K., Marshall, T. R., & Kievit, R. A. (2019). Raincloud plots: A  
780 multi-platform tool for robust data visualization. *Wellcome Open Research*, 4.

781 Arnal, L. H. (2012). Predicting “When” Using the Motor System’s Beta-Band Oscillations. *Front*  
782 *Hum Neurosci*, 6, 225. <https://doi.org/10.3389/fnhum.2012.00225>

783 Arnal, L. H., & Giraud, A. L. (2012). Cortical oscillations and sensory predictions. *Trends in*  
784 *cognitive sciences*, 16(7), 390-398.

785 Austin, P. (2001). Word order in a free word order language: the case of Jiwari. *Forty years on: Ken*  
786 *Hale and Australian languages*, 2057323.

787 Austin, P. C., & Hux, J. E. (2002). A brief note on overlapping confidence intervals. *Journal of*  
788 *Vascular Surgery*, 36(1), 194–195.

789 Baayen, H., Vasishth, S., Kliegl, R., & Bates, D. (2017). The cave of shadows: Addressing the human  
790 factor with generalized additive mixed models. *Journal of Memory and Language*, 94, 206–  
791 234.

792 Baayen, R. H., Davidson, D. J., & Bates, D. M. (2008). Mixed-effects modeling with crossed random  
793 effects for subjects and items. *Journal of Memory and Language*, 59(4), 390–412.

794 Bastiaansen, M. C., Van Berkum, J. J., & Hagoort, P. (2002). Syntactic processing modulates the  $\theta$   
795 rhythm of the human EEG. *Neuroimage*, 17(3), 1479–1492.

796 Bastiaansen, M., Magyari, L., & Hagoort, P. (2010). Syntactic unification operations are reflected in  
797 oscillatory dynamics during on-line sentence comprehension. *Journal of Cognitive*  
798 *Neuroscience*, 22(7), 1333-1347.

799 Bastos, A. M., Usrey, W. M., Adams, R. A., Mangun, G. R., Fries, P., & Friston, K. J. (2012).  
800 Canonical microcircuits for predictive coding. *Neuron*, 76(4), 695-711.

801 Bates, D., Maechler, M., Bolker, B., Walker, S., Christensen, R. H. B., Singmann, H., Dai, B.,  
802 Grothendieck, G., Green, P., & Bolker, M. B. (2015). Package ‘lme4.’ *Convergence*, 12(1), 2.

803 Bates, E., Devescovi, A., & Wulfeck, B. (2001). Psycholinguistics: A Cross-Language Perspective.  
804 *Annual Review of Psychology*, 52(1), 27.

805 Bell, A. J., & Sejnowski, T. J. (1995). An information-maximization approach to blind separation and  
806 blind deconvolution. *Neural Computation*, 7(6), 1129–1159.

807 Bonhage, C. E., Meyer, L., Gruber, T., Friederici, A. D., & Mueller, J. L. (2017). Oscillatory EEG  
808 dynamics underlying automatic chunking during sentence processing. *Neuroimage*, 152, 647-  
809 657. doi: <https://doi.org/10.1016/j.neuroimage.2017.03.018>

810 Bornkessel-Schlesewsky, I., Kretzschmar, F., Tune, S., Wang, L., Genc, S., Philipp, M., Roehm, D.,  
811 & Schlesewsky, M. (2011). Think globally: Cross-linguistic variation in electrophysiological  
812 activity during sentence comprehension. *Brain Lang*, 117(3), 133–152.  
813 <https://doi.org/10.1016/j.bandl.2010.09.010>

814 Bornkessel-Schlesewsky, I., Schlesewsky, M., Small, S. L., & Rauschecker, J. P. (2015).  
815 Neurobiological roots of language in primate audition: Common computational properties.  
816 *Trends Cogn Sci*, 19(3), 142–150. <https://doi.org/10.1016/j.tics.2014.12.008>

817 Bornkessel, I., & Schlesewsky, M. (2006). The extended argument dependency model: A  
818 neurocognitive approach to sentence comprehension across languages. *Psychol Rev*, 113(4),  
819 787–821. <https://doi.org/10.1037/0033-295X.113.4.787>

820 Bressler, S. L., & Richter, C. G. (2015). Interareal oscillatory synchronization in top-down neocortical  
821 processing. *Current Opinion in Neurobiology*, 31, 62–66. doi:  
822 <https://doi.org/10.1016/j.conb.2014.08.010>

823 Cao, Y., Oostenveld, R., Alday, P. M., & Piai, V. (2022). Are alpha and beta oscillations spatially  
824 dissociated over the cortex in context-driven spoken-word production?. *Psychophysiology*,  
825 e13999. doi: <https://doi.org/10.1111/psyp.13999>

826 Chapeton, J. I., Haque, R., Wittig, J. H., Inati, S. K., & Zaghloul, K. A. (2019). Large-Scale  
827 Communication in the Human Brain Is Rhythmically Modulated through Alpha Coherence.  
828 *Curr Biol*, 29(17), 2801-2811 e5. <https://doi.org/10.1016/j.cub.2019.07.014>

829 Claus O. Wilke, C.O. (2019). cowplot: Streamlined Plot Theme and Plot Annotations for 'ggplot2'. R  
830 package version 1.0.0. <https://CRAN.R-project.org/package=cowplot>

831 Cohen, M. R., & Maunsell, J. H. (2011). Using neuronal populations to study the mechanisms  
832 underlying spatial and feature attention. *Neuron*, 70(6), 1192-1204.

833 Corcoran, A. W., Alday, P. M., Schlesewsky, M., & Bornkessel-Schlesewsky, I. (2018). Toward a  
834 reliable, automated method of individual alpha frequency (IAF) quantification.  
835 *Psychophysiology*, 55(7), e13064. <https://doi.org/10.1111/psyp.13064>

836 Corcoran, A. W., Macefield, V. G., & Hohwy, J. (2021). Be still my heart: Cardiac regulation as a  
837 mode of uncertainty reduction. *Psychonomic Bulletin & Review*, 28, 1211–1223. doi:  
838 <https://doi.org/10.3758/s13423-021-01888-y>

839 Corcoran, A. W., Perera, R., Koroma, M., Kouider, S., Hohwy, H., Andrillon, T. (2022). Expectations  
840 boost the reconstruction of auditory features from electrophysiological responses to noisy  
841 speech, *Cerebral Cortex*. doi: <https://doi.org/10.1093/cercor/bhac094>

842 Corcoran, A.W., Alday, P.M., Schlesewsky, M., & Bornkessel-Schlesewsky, I. (2019). restingIAF  
843 (v1.0.3). Retrieved from <https://github.com/corcorana/restingIAF>

844 Crivelli-Decker, J., Hsieh, L. T., Clarke, A., & Ranganath, C. (2018). Theta oscillations promote  
845 temporal sequence learning. *Neurobiol Learn Mem*.  
846 <https://doi.org/10.1016/j.nlm.2018.05.001>

847 Cross, Z. R., Helfrich, R. F., Kohler, M. J., Corcoran, A. W., Coussens, S., Zou-Williams, L.,  
848 Schlesewsky, M., Gaskell, M. G., Knight, R. T., & Bornkessel-Schlesewsky, I. (2021).  
849 Spindle-slow oscillation coupling during sleep predicts sequence-based language learning.  
850 *BioRxiv*. doi: <https://doi.org/10.1101/2020.02.13.948539>

851 Cross, Z. R., Corcoran, A. W., Kohler, M. J., Schlesewsky, M., & Bornkessel-Schlesewsky, I. (2022,  
852 March 27). Oscillatory and aperiodic neural activity jointly predict language learning.  
853 Retrieved from osf.io/7yr46.

854 Cross, Z. R., Kohler, M. J., Schlesewsky, M., Gaskell, M. G., & Bornkessel-Schlesewsky, I. (2018).  
855 Sleep-dependent memory consolidation and incremental sentence comprehension:  
856 computational dependencies during language learning as revealed by neuronal oscillations.  
857 *Frontiers in Human Neuroscience*, 12. <https://doi.org/10.3389/fnhum.2018.00018>

858 Cross, Z. R., Santamaria, A., Corcoran, A. W., Chatburn, A., Alday, P. M., Coussens, S., & Kohler,  
859 M. J. (2020b). Individual alpha frequency modulates sleep-related emotional memory  
860 consolidation. *Neuropsychologica*, 148. doi: <https://doi.org/10.1101/202176>

861 Cross, Z. R., Zou-Williams, L., Wilkinson, E., Schlesewsky, M., & Bornkessel-Schlesewsky, I.  
862 (2020a). Mini Pinyin: A modified miniature language for studying language learning and  
863 incremental sentence processing. *Behavior Research Methods*. doi:  
864 <https://doi.org/10.3758/s13428-020-01473-6>

865 Dave, S., Brothers, T. A., & Swaab, T. Y. (2018). 1/f neural noise and electrophysiological indices of  
866 contextual prediction in aging. *Brain Res*, 1691, 34–43.  
867 <https://doi.org/10.1016/j.brainres.2018.04.007>

868 Davidson, D. J., & Indefrey, P. (2007). An inverse relation between event-related and time–frequency  
869 violation responses in sentence processing. *Brain Research*, 1158, 81–92.

870 de Diego-Balaguer, R., Fuentemilla, L., & Rodriguez-Fornells, A. (2011). Brain Dynamics Sustaining  
871 Rapid Rule Extraction from Speech. *J Cogn Neurosci*, 23(10), 3105–3120.

872 de Vries, I. E. J., Slagter, H. A., & Olivers, C. N. L. (2020). Oscillatory Control over Representational  
873 States in Working Memory. *Trends Cogn Sci*, 24(2), 150–162.  
874 <https://doi.org/10.1016/j.tics.2019.11.00>

875 Donoghue, T., Dominguez, J., & Voytek, B. (2020). Electrophysiological frequency band ratio  
876 measures conflate periodic and aperiodic neural activity. *Eneuro*, 7(6). doi:  
877 <https://doi.org/10.1523/ENEURO.0192-20.2020>

878 Donoghue, T., Haller, M., Peterson, E. J., Varma, P., Sebastian, P., Gao, R., ... & Voytek, B. (2020).  
879 Parameterizing neural power spectra into periodic and aperiodic components. *Nature  
880 Neuroscience*, 23(12), 1655–1665. doi: <https://doi.org/10.1038/s41593-020-00744-x>

881 Donoghue, T., Schawronkow, N., & Voytek, B. (2021). Methodological considerations for studying  
882 neural oscillations. *European Journal of Neuroscience*. doi: <https://doi.org/10.1111/ejn.15361>

883 Doppelmayr, M., Klimesch, W., Pachinger, T., & Ripper, B. (1998). Individual differences in brain  
884 dynamics: important implications for the calculation of event-related band power. *Biological  
885 Cybernetics*, 79(1), 49–57.

886 Dziego, C., Bornkessel-Schlesewsky, I., Jano, S., Chatburn, A., Schlesewsky, M., Immink, M. A., ...  
887 & Cross, Z. R. (2022). Neural and cognitive correlates of performance in dynamic multi-  
888 modal settings. *bioRxiv*. doi: <https://doi.org/10.1101/2022.03.23.485424>

889 Engel, A. K., Fries, P., & Singer, W. (2001). Dynamic predictions: Oscillations and synchrony in top-  
890 down processing. *Nature Reviews Neuroscience*, 2, 12.

891 Eschmann, K. C., Bader, R., & Mecklinger, A. (2020). Improving episodic memory: Frontal-midline  
892 theta neurofeedback training increases source memory performance. *NeuroImage*, 222,  
893 117219.

894 Fasiolo, M., Nedellec, R., Goude, Y., & Wood, S. N. (2019). Scalable visualization methods for  
895 modern generalized additive models. *Journal of Computational and Graphical Statistics*, 1–9.

896 Fellner, M. C., Gollwitzer, S., Rampp, S., Kreiselmeyr, G., Bush, D., Diehl, B., Axmacher, N.,  
897 Hamer, H., & Hanslmayr, S. (2019). Spectral fingerprints or spectral tilt? Evidence for  
898 distinct oscillatory signatures of memory formation. *PLoS Biol*, 17(7), e3000403.  
899 <https://doi.org/10.1371/journal.pbio.3000403>

900 Fox, J., Weisberg, S., Adler, D., Bates, D., Baud-Bovy, G., Ellison, S., & Heilberger, R. (2011).  
901 *Package “car”: Companion to applied regression*.

902 Friston, K. (2010). The free-energy principle: A unified brain theory? *Nat Rev Neurosci*, 11(2), 127–  
903 138. <https://doi.org/10.1038/nrn2787>

904 Friston, K. (2018). Does predictive coding have a future? *Nature Neuroscience*, 21(8), 1019–1021.

905 Friston, K. J. (2019). Waves of prediction. *PLoS Biol*, 17(10), e3000426.  
906 <https://doi.org/10.1371/journal.pbio.3000426>

907 Gallotto, S., Duecker, F., ten Oever, S., Schuhmann, T., de Graaf, T. A., & Sack, A. T. (2020).  
908 Relating alpha power modulations to competing visuospatial attention theories. *NeuroImage*,  
909 207, 116429.

910 Gao, R., Peterson, E. J., & Voytek, B. (2017). Inferring synaptic excitation/inhibition balance from  
911 field potentials. *Neuroimage*, 158, 70-78. doi: 10.1016/j.neuroimage.2017.06.078

912 Gerster, M., Waterstraat, G., Litvak, V., Lehnertz, K., Schnitzler, A., Florin, E., ... & Nikulin, V.  
913 (2022). Separating neural oscillations from aperiodic 1/f activity: challenges and  
914 recommendations. *Neuroinformatics*, 1-22.

915 Griffiths, B. J., Mayhew, S. D., Mullinger, K. J., Jorge, J., Charest, I., Wimber, M., & Hanslmayr, S.  
916 (2019). Alpha/beta power decreases track the fidelity of stimulus-specific information. *eLife*,  
917 8. <https://doi.org/10.7554/eLife.49562>

918 Guderian, S., & Düzel, E. (2005). Induced theta oscillations mediate large-scale synchrony with  
919 mediotemporal areas during recollection in humans. *Hippocampus*, 15(7), 901–912.

920 Hanslmayr, S., & Staudigl, T. (2014). How brain oscillations form memories—A processing based  
921 perspective on oscillatory subsequent memory effects. *Neuroimage*, 85 Pt 2, 648–655.  
922 <https://doi.org/10.1016/j.neuroimage.2013.05.121>

923 Harris, K. D., & Thiele, A. (2011). Cortical state and attention. *Nature Reviews Neuroscience*, 12(9),  
924 509-523.

925 Hastie, T., & Tibshirani, R. (1987). Generalized additive models: Some applications. *Journal of the  
926 American Statistical Association*, 82(398), 371–386.

927 Hastie, T., & Tibshirani, R. (1990). Exploring the nature of covariate effects in the proportional  
928 hazards model. *Biometrics*, 1005–1016.

929 He, B. J. (2014). Scale-free brain activity: Past, present, and future. *Trends Cogn Sci*, 18(9), 480–487.  
930 <https://doi.org/10.1016/j.tics.2014.04.003>

931 He, B. J., Zempel, J. M., Snyder, A. Z., & Raichle, M. E. (2010). The temporal structures and  
932 functional significance of scale-free brain activity. *Neuron*, 66(3), 353–369.  
933 <https://doi.org/10.1016/j.neuron.2010.04.020>

934 Herweg, N. A., Solomon, E. A., & Kahana, M. J. (2020). Theta Oscillations in Human Memory.  
935 *Trends Cogn Sci*, 24(3), 208–227. <https://doi.org/10.1016/j.tics.2019.12.006>

936 Immink, M. A., Cross, Z. R., Chatburn, A., Baumeister, J., Schlesewsky, M., & Bornkessel-  
937 Schlesewsky, I. (2021). Resting-state aperiodic neural dynamics predict individual differences  
938 in visuomotor performance and learning. *Human Movement Science*, 78, 102829. doi:  
939 <https://doi.org/10.1016/j.humov.2021.102829>

940 Kassambara, A. (2020). ggpubr: 'ggplot2' Based Publication Ready Plots. R package version 0.4.0.  
941 <https://CRAN.R-project.org/package=ggpubr>

942 Kaufeld, G., Bosker, H. R., Alday, P. M., Meyer, A. S., & Martin, A. E. (2020). Linguistic structure  
943 and meaning organize neural oscillations into a content-specific hierarchy. *BioRxiv*,  
944 2020.02.05.935676. <https://doi.org/10.1101/2020.02.05.935676>

945 Keitel, A., & Gross, J. (2016). Individual Human Brain Areas Can Be Identified from Their  
946 Characteristic Spectral Activation Fingerprints. *PLoS Biol*, 14(6), e1002498.  
947 <https://doi.org/10.1371/journal.pbio.1002498>

948 Kepinska, O., Pereda, E., Caspers, J., & Schiller, N. O. (2017). Neural oscillatory mechanisms during  
949 novel grammar learning underlying language analytical abilities. *Brain Lang*, 175, 99–110.  
950 <https://doi.org/10.1016/j.bandl.2017.10.003>

951 Khader, P. H., Jost, K., Ranganath, C., & Rösler, F. (2010). Theta and alpha oscillations during  
952 working-memory maintenance predict successful long-term memory encoding. *Neuroscience  
953 letters*, 468(3), 339-343.

954 Kiolar, A., Meltzer, J. A., Moreno, S., Alain, C., & Bialystok, E. (2014). Oscillatory responses to  
955 semantic and syntactic violations. *Journal of Cognitive Neuroscience*, 26(12), 2840-2862.

956 Kikuchi, Y., Sedley, W., Griffiths, T. D., & Petkov, C. I. (2018). Evolutionarily conserved neural  
957 signatures involved in sequencing predictions and their relevance for language. *Current  
958 Opinion in Behavioral Sciences*, 21, 145–153. <https://doi.org/10.1016/j.cobeha.2018.05.002>

959 Klimesch, W. (2013). An algorithm for the EEG frequency architecture of consciousness and brain  
960 body coupling. *Frontiers in human neuroscience*, 7, 766. doi:  
961 <https://doi.org/10.3389/fnhum.2013.00766>

962 Klimesch, W., Freunberger, R., & Sauseng, P. (2010). Oscillatory mechanisms of process binding in  
963 memory. *Neuroscience & Biobehavioral Reviews*, 34(7), 1002–1014.

964 Klimesch, W., Freunberger, R., Sauseng, P., & Gruber, W. (2008). A short review of slow phase  
965 synchronization and memory: Evidence for control processes in different memory systems?  
966 *Brain Res*, 1235, 31–44. <https://doi.org/10.1016/j.brainres.2008.06.049>

967 Klimesch, W.. (2012). Alpha-band oscillations, attention, and controlled access to stored information.  
968 *Trends in Cognitive Sciences*, 16(12), 606–617. <http://dx.doi.org/10.1016/j.tics.2012.10.007>

969 Kosciessa, J. Q., Grandy, T. H., Garrett, D. D., & Werkle-Bergner, M. (2020). Single-trial  
970 characterization of neural rhythms: Potential and challenges. *NeuroImage*, 206, 116331. doi:  
971 <https://doi.org/10.1016/j.neuroimage.2019.116331>

972 Kuznetsova, A., Brockhoff, P. B., & Christensen, R. H. B. (2017). lmerTest package: Tests in linear  
973 mixed effects models. *Journal of Statistical Software*, 82(13).

974 Lam, N. H., Schoffelen, J. M., Udden, J., Hulten, A., & Hagoort, P. (2016). Neural activity during  
975 sentence processing as reflected in theta, alpha, beta, and gamma oscillations. *Neuroimage*.  
976 <https://doi.org/10.1016/j.neuroimage.2016.03.007>

977 Lendner, J. D., Helfrich, R. F., Mander, B. A., Romundstad, L., Lin, J. J., Walker, M. P., Larsson, P.  
978 G., & Knight, R. T. (2020). An electrophysiological marker of arousal level in humans. *eLife*.  
979 doi: 10.7554/eLife.55092

980 Lewis, A. G., & Bastiaansen, M. (2015). A predictive coding framework for rapid neural dynamics  
981 during sentence-level language comprehension. *Cortex*, 68, 155–168.  
982 <https://doi.org/10.1016/j.cortex.2015.02.014>

983 Lewis, A. G., Lemhöfer, K., Schoffelen, J. M., & Schriefers, H. (2016). Gender agreement violations  
984 modulate beta oscillatory dynamics during sentence comprehension: A comparison of second  
985 language learners and native speakers. *Neuropsychologia*, 89, 254-272. doi:  
986 <https://doi.org/10.1016/j.neuropsychologia.2016.06.031>

987 Lewis, A. G., Schoffelen, J. M., Schriefers, H., & Bastiaansen, M. (2016). A predictive coding  
988 perspective on beta oscillations during sentence-level language comprehension. *Frontiers in  
989 human neuroscience*, 10, 85.

990 Lewis, A. G., Wang, L., & Bastiaansen, M. (2015). Fast oscillatory dynamics during language  
991 comprehension: Unification versus maintenance and prediction? *Brain and language*, 148,  
992 51-63.

993 Lin, X., & Zhang, D. (1999). Inference in generalized additive mixed models by using smoothing  
994 splines. *Journal of the Royal Statistical Society: Series b (Statistical Methodology)*, 61(2),  
995 381–400.

996 Lüdecke, D. (2018). “ggeffects: Tidy Data Frames of Marginal Effects from Regression  
997 Models.” *Journal of Open Source Software*, \*3\*(26), 772. doi: 10.21105/joss.00772  
998 (URL:<https://doi.org/10.21105/joss.00772>).

999 Luft, C. D. B. (2014). Learning from feedback: the neural mechanisms of feedback processing  
1000 facilitating better performance. *Behavioural brain research*, 261, 356-368.

1001 Luft, C. D. B., Takase, E., & Bhattacharya, J. (2014). Processing graded feedback:  
1002 electrophysiological correlates of learning from small and large errors. *Journal of cognitive*  
1003 *neuroscience*, 26(5), 1180-1193.

1004 MacGregor-Fors, I., & Payton, M. E. (2013). Contrasting diversity values: Statistical inferences based  
1005 on overlapping confidence intervals. *PLoS One*, 8(2).

1006 MacWhinney, B., Bates, E., & Kliegl, R. (1984). Cue validity and sentence interpretation in English,  
1007 German, and Italian. *Journal of Verbal Learning and Verbal Behavior*, 23(2), 127–150.  
1008 [http://dx.doi.org/10.1016/S0022-5371\(84\)90093-8](http://dx.doi.org/10.1016/S0022-5371(84)90093-8)

1009 Mai, G., Minett, J. W., & Wang, W. S. Y. (2016). Delta, theta, beta, and gamma brain oscillations  
1010 index levels of auditory sentence processing. *Neuroimage*, 133, 516-528. doi:  
1011 <https://doi.org/10.1016/j.neuroimage.2016.02.064>

1012 Marra, G., & Wood, S. N. (2011). Practical Variable Selection for Generalized Additive Models.  
1013 *Computational Statistics & Data Analysis*, 55, 2372–2387.

1014 Martin, A. E. (2016). Language Processing as Cue Integration: Grounding the Psychology of  
1015 Language in Perception and Neurophysiology. *Frontiers in Psychology*, 7, 120.  
1016 <https://doi.org/10.3389/fpsyg.2016.00120>

1017 Mathot, S., Schreij, D., & Theeuwes, J. (2012). OpenSesame: An open-source, graphical experiment  
1018 builder for the social sciences. *Behav Res Methods*, 44(2), 314–324.  
1019 <https://doi.org/10.3758/s13428-011-0168-7>

1020 Meyer, L., Obleser, J., & Friederici, A. D. (2013). Left parietal alpha enhancement during working  
1021 memory-intensive sentence processing. *Cortex*, 49(3), 711-721.

1022 Mormann, F., Fell, J., Axmacher, N., Weber, B., Lehnertz, K., Elger, C. E., & Fernández, G. (2005).  
1023 Phase/amplitude reset and theta–gamma interaction in the human medial temporal lobe during  
1024 a continuous word recognition memory task. *Hippocampus*, 15(7), 890–900.

1025 Mueller, J. L., Hahne, A., Fujii, Y., & Friederici, A. D. (2005). Native and nonnative speakers'  
1026 processing of a miniature version of Japanese as revealed by ERPs. *Journal of Cognitive*  
1027 *Neuroscience*, 17(8), 1229-1244.

1028 Muthukumaraswamy, S. D., & Liley, D. T. (2018). 1/f electrophysiological spectra in resting and  
1029 drug-induced states can be explained by the dynamics of multiple oscillatory relaxation  
1030 processes. *Neuroimage*, 179, 582–595.

1031 Nenadic, O., & Greenacre, M. (2007). Correspondence analysis in R, with two-and three-dimensional  
1032 graphics: The ca package. *Journal of Statistical Software*, 20(3).

1033 Oostenveld, R., Fries, P., Maris, E., & Schoffelen, J.-M. (2011). FieldTrip: Open source software for  
1034 advanced analysis of MEG, EEG, and invasive electrophysiological data. *Computational  
1035 Intelligence and Neuroscience, 2011*.

1036 Osipova, D., Takashima, A., Oostenveld, R., Fernandez, G., Maris, E., & Jensen, O. (2006). Theta  
1037 and gamma oscillations predict encoding and retrieval of declarative memory. *J Neurosci,*  
1038 26(28), 7523–7531. <https://doi.org/10.1523/JNEUROSCI.1948-06.2006>

1039 Ouyang, G., Hildebrandt, A., Schmitz, F., & Herrmann, C. S. (2020). Decomposing alpha and 1/f  
1040 brain activities reveals their differential associations with cognitive processing speed.  
1041 *Neuroimage, 205*, 116304. <https://doi.org/10.1016/j.neuroimage.2019.116304>

1042 Parish, G., Hanslmayr, S., & Bowman, H. (2018). The Sync/deSync Model: How a Synchronized  
1043 Hippocampus and a Desynchronized Neocortex Code Memories. *J Neurosci, 38*(14), 3428–  
1044 3440. <https://doi.org/10.1523/JNEUROSCI.2561-17.201>

1045 Pedersen, E. J., Miller, D. L., Simpson, G. L., & Ross, N. (2019). Hierarchical generalized additive  
1046 models in ecology: An introduction with mgcv. *PeerJ, 7*, e6876.

1047 Perrin, F., Pernier, J., Bertrand, O., & Echallier, J. F. (1989). Spherical splines for scalp potential and  
1048 current density mapping. *Electroencephalography and Clinical Neurophysiology, 72*(2), 184–  
1049 187.

1050 Peterson, E. J., Rosen, B. Q., Campbell, A. M., Belger, A., & Voytek, B. (2017). 1/f neural noise is a  
1051 better predictor of schizophrenia than neural oscillations. *BioRxiv, 113449*.

1052 Prat, C. S., Yamasaki, B. L., Kluender, R. A., & Stocco, A. (2016). Resting-state qEEG predicts rate  
1053 of second language learning in adults. *Brain & Language, 157*, 44-50. doi:  
1054 <https://doi.org/10.1016/j.bandl.2016.04.007>

1055 Richter, C. G., Thompson, W. H., Bosman, C. A., & Fries, P. (2017). Top-down beta enhances  
1056 bottom-up gamma. *The Journal of Neuroscience, 37*(28), 6698-6711. doi:  
1057 10.1523/JNEUROSCI.3771-16.2017

1058 Robertson, M. M., Furlong, S., Voytek, B., Donoghue, T., Boettiger, C. A., & Sheridan, M. A. (2019).  
1059 EEG power spectral slope differs by ADHD status and stimulant medication exposure in early  
1060 childhood. *Journal of Neurophysiology, 122*(6), 2427-2437. doi:  
1061 <https://doi.org/10.1152/jn.00388.2019>

1062 Rossi, E., & Prystauka, Y. (2020). Oscillatory brain dynamics of pronoun processing in native  
1063 Spanish speakers and in late second language learners of Spanish. *Bilingualism: Language  
1064 and Cognition, 23*(5), 964-977. doi: <https://doi.org/10.1017/S1366728919000798>

1065 Samaha, J., Bauer, P., Cimaroli, S., & Postle, B. R. (2015). Top-down control of the phase of alpha-  
1066 band oscillations as a mechanism for temporal prediction. *PNAS, 112*(27), 8439-8444. doi:  
1067 <https://doi.org/10.1073/pnas.1503686112>

1068 Sarkar, D. (2008). *Lattice: Multivariate data visualization with R*. Springer Science & Business  
1069 Media.

1070 Sauppe, S., Choudhary, K. K., Giroud, N., Blasi, D. E., Norcliffe, E., Bhattacharya, S., ... & Bickel,  
1071 B. (2021). Neural signatures of syntactic variation in speech planning. *PLoS Biology*, 19(1),  
1072 e3001038. doi: <https://doi.org/10.1371/journal.pbio.3001038>

1073 Schad, D. J., Vasishth, S., Hohenstein, S., & Kliegl, R. (2020). How to capitalize on a priori contrasts  
1074 in linear (mixed) models: A tutorial. *Journal of Memory and Language*, 110, 104038.

1075 Schreiner, T., Goldi, M., & Rasch, B. (2015). Cueing vocabulary during sleep increases theta activity  
1076 during later recognition testing. *Psychophysiology*, 52(11), 1538–1543.  
1077 <https://doi.org/10.1111/psyp.12505>

1078 Sheehan, T. C., Sreekumar, V., Inati, S. K., & Zaghloul, K. A. (2018). Signal Complexity of Human  
1079 Intracranial EEG Tracks Successful Associative-Memory Formation across Individuals. *J  
1080 Neurosci*, 38(7), 1744–1755. <https://doi.org/10.1523/JNEUROSCI.2389-17.2017>

1081 Siegel, M., Donner, T. H., & Engel, A. K. (2012). Spectral fingerprints of large-scale neuronal  
1082 interactions. *Nat Rev Neurosci*, 13(2), 121–134. <https://doi.org/10.1038/nrn313>

1083 Stokes, M., & Spaak, E. (2016). The importance of single-trial analyses in cognitive neuroscience.  
1084 Trends in Cognitive Sciences, 20(7), 483-486. doi: <https://doi.org/10.1016/j.tics.2016.05.008>

1085 Tan, H., Jenkinson, N., & Brown, P. (2014). Dynamic neural correlates of motor error monitoring and  
1086 adaptation during trial-to-trial learning. *Journal of Neuroscience*, 34(16), 5678-5688.

1087 Thuwal, K., Banerjee, A., & Roy, D. (2021). Aperiodic and periodic components of ongoing  
1088 oscillatory brain dynamics link distinct functional aspects of cognition across adult  
1089 lifespan. *Eneuro*, 8(5). doi: 10.1523/ENEURO.0224-21.2021

1090 van Rij, J., Wieling, M., Baayen, R. H., van Rijn, H., & van Rij, M. J. (2016). Package ‘itsadug.’  
1091 Voytek, B., Kramer, M. A., Case, J., Lepage, K. Q., Tempesta, Z. R., Knight, R. T., & Gazzaley, A.  
1092 (2015). Age-Related Changes in 1/f Neural Electrophysiological Noise. *J Neurosci*, 35(38),  
1093 13257–13265. <https://doi.org/10.1523/JNEUROSCI.2332-14.2015>

1094 Wang, P., Maye, A., Daume, J., Xue, G., & Engel, A. K. (2019). Dynamic Predictions: Oscillatory  
1095 Mechanisms Underlying Multisensory Sequence Processing. *BioRxiv*, 778969.

1096 Waschke, L., Donoghue, T., Fiedler, L., Smith, S., Garrett, D. D., Voytek, B., & Obleser, J. (2021).  
1097 Modality-specific tracking of attention and sensory statistics in the human  
1098 electrophysiological spectral exponent. *Elife*, 10, e70068. doi: 10.7554/eLife.70068

1099 Watrous, A. J., Fell, J., Ekstrom, A. D., & Axmacher, N. (2015). More than spikes: Common  
1100 oscillatory mechanisms for content specific neural representations during perception and  
1101 memory. *Curr Opin Neurobiol*, 31, 33–39. <https://doi.org/10.1016/j.conb.2014.07.024>

1102 Welch, P. (1967) The Use of Fast Fourier Transform for the Estimation of Power Spectra: A Method  
1103 Based on Time Averaging Over Short, Modified Periodograms. *IEEE Transactions on Audio  
1104 and Electroacoustics*, 15, 70-73. doi: <http://dx.doi.org/10.1109/TAU.1967.1161901>

1105 Wen, H., & Liu, Z. (2016). Separating fractal and oscillatory components in the power spectrum of  
1106 neurophysiological signal. *Brain Topography*, 29(1), 13–26.

1107 Wickham, H., Averick, M., Bryan, J., Chang, W., McGowan, L., François, R., Grolemund, G., Hayes,  
1108 A., Henry, L., & Hester, J. (2019). Welcome to the Tidyverse. *Journal of Open Source  
Software*, 4(43), 1686.

1110 Womelsdorf, T., Valiante, T. A., Sahin, N. T., Miller, K. J., & Tiesinga, P. (2014). Dynamic circuit  
1111 motifs underlying rhythmic gain control, gating and integration. *Nat Neurosci*, 17(8), 1031–  
1112 1039. <https://doi.org/10.1038/nn.376>

1113 Wood, S. (2006). *R-Manual: The MGCV package*. Version 1.3–22. Technical Report.

1114 Wood, S. N. (2003). Thin plate regression splines. *Journal of the Royal Statistical Society, Series B*  
1115 65, 95–114.

1116 Wood, S. N. (2013). A simple test for random effects in regression models. *Biometrika* 100(4), 1005–  
1117 1010.

1118 Wood, S. N. (2017). *Generalized additive models: An introduction with R*. 2nd ed. Boca Raton, FL:  
1119 CRC Press

1120 Wood, S. N., Scheipl, F., & Faraway, J. J. (2013). Straightforward intermediate  
rank tensor product smoothing in mixed models. *Stat. Comput.* 23, 341–360.